

Associate Editor comments:

Comments to the Author:

In the light of the positive assessment of the revised manuscript by the referee, I'm happy to offer publication of your manuscript in Biogeosciences. Note that this offer is conditional on revising the minor issues noted by the referee. Also, I agree with the referee that especially the discussion should be edited to further enhance its readability. Looking forward to the revised manuscript,

Thank you for the encouraging comments and giving us an opportunity to revise our manuscript. We addressed all the comments and make some edits and corrections as well.

Referee #2

The authors have made thorough work in revising the MS and well addressed my comments. Thanks for scientific discussion!

Thank you for your all nice comments and We are happy we addressed all your comments.

I suggest the MS can be published after proof-reading. I encourage the authors to check whether part of their additions (in red) into Discussion could be shortened.

Thank you for your suggestion! We double checked the Discussion part, made some changes and got rid of one paragraph to make it more readable.

Few remarks: L145: ORCHIDEE, L615: capture processes, L913: citation missing!

We changed 'ORCHIFEE' to 'ORCHIDEE' (L141) and added the citation of Williams and Flanagan, 1998 (L877). But for L 615 'capture processes', we double check the last version of manuscript and didn't capture what kind of response we should give

1 Extending a land-surface model with *Sphagnum* moss to simulate responses
2 of a northern temperate bog to whole-ecosystem warming and elevated CO₂

Formatted: Font: Italic

3
4 Xiaoying Shi^{1*}, Daniel M. Ricciuto¹, Peter E. Thornton¹, Xiaofeng Xu², Fengming Yuan¹,
5 Richard J. Norby¹, Anthony P. Walker¹, Jeffrey Warren¹, Jiafu Mao¹, Paul J. Hanson¹,
6 Lin Meng³, David Weston¹, Natalie A. Griffiths¹

7 ¹Climate Change Science Institute and Environmental Sciences Division, Oak Ridge
8 National Laboratory, Oak Ridge, TN 37831, USA

9 ²Biology Department San Diego State University, San Diego, CA, 92182-4614, USA

10
11 ³Department of Geological and Atmospheric Sciences, Iowa State University, Ames, IA,
12 50011

13
14

15 *To whom correspondence should be addressed

16 Corresponding author's email: shix@ornl.gov

17 Fax: 865-574-2232

18

19
20
21
22
23
24
25
26
27
28
29
30
31
32
33
34
35
36
37
38
39

40 **Abstract**

41 Mosses need to be incorporated into Earth system models to better simulate
42 peatland functional dynamics under changing environment. *Sphagnum* mosses are strong
43 determinants of nutrient, carbon and water cycling in peatland ecosystems. However,
44 most land surface models do not include *Sphagnum* or other mosses as represented plant
45 functional types (PFTs), thereby limiting predictive assessment of peatland responses to
46 environmental change. In this study, we introduce a moss PFT into the land model
47 component (ELM) of the Energy Exascale Earth System Model (E3SM), by developing
48 water content dynamics and non-vascular photosynthetic processes for moss. The model
49 was parameterized and independently evaluated against observations from an
50 ombrotrophic forested bog as part of the Spruce and Peatland Responses Under Changing
51 Environments (SPRUCE) project. Inclusion of a *Sphagnum* PFT with some *Sphagnum*
52 specific processes in ELM allows it to capture the observed seasonal dynamics of
53 *Sphagnum* gross primary production (GPP), albeit with an underestimate of peak GPP.
54 The model simulated a reasonable annual net primary production (NPP) for moss but
55 with less interannual variation than observed, and reproduced above ground biomass for
56 tree PFTs and stem biomass for shrubs. Different species showed highly variable
57 warming responses under both ambient and elevated atmospheric CO₂ concentrations,
58 and elevated CO₂ altered the warming response direction for the peatland ecosystem.
59 Microtopography is critical: *Sphagnum* mosses on hummocks and hollows were
60 simulated to show opposite warming responses (NPP decreasing with warming on
61 hummocks, but increasing in hollows), and hummock *Sphagnum* was modeled to have
62 strong dependence on water table height. Inclusion of this new moss PFT in global ELM
63

64 simulations may provide a useful foundation for the investigation of northern peatland
65 carbon exchange, enhancing the predictive capacity of carbon dynamics across the
66 regional and global scales.

67 **Copyright statement**

68 This manuscript has been authored by UT-Battelle, LLC under Contract No. DE-
69 AC05-00OR22725 with the U.S. Department of Energy. The United States Government
70 retains and the publisher, by accepting the article for publication, acknowledges that the
71 United States Government retains a non-exclusive, paid-up, irrevocable, world-wide
72 license to publish or reproduce the published form of this manuscript, or allow others to
73 do so, for United States Government purposes. The Department of Energy will provide
74 public access to these results of federally sponsored research in accordance with the DOE
75 Public Access Plan (<http://energy.gov/downloads/doe-public-access-plan>).

76 77 **1. Introduction**

78 Boreal peatlands store at least 500 Pg of soil carbon due to incomplete
79 decomposition of plant litter inputs resulting from a combination of low temperature and
80 water-saturated soils. Because of this capacity to store carbon, boreal peatlands have
81 played a critical role in regulating the global climate since the onset of the Holocene
82 (Frolking and Roulet, 2007; Yu et al., 2010). The total carbon stock is large but
83 uncertain: a new estimation of northern peatlands carbon stock of 1055 Pg was recently
84 reported by Nichols and Peteet (2019). The rapidly changing climate at high latitudes is
85 likely to impact both primary production and decomposition rates in peatlands,
86 contributing to uncertainty in whether peatlands will continue their function as net carbon
87

88 sinks in the long term (Moore et al., 1998; Turetsky et al., 2002; Wu and Roulet, 2014).
89 Manipulative experiments and process-based models are thus needed to make defensible
90 projections of net carbon balance of northern peatlands under anticipated global warming
91 (Hanson et al, 2017; Shi et al., 2015).

92 Peatlands are characterized by a ground layer of bryophytes, and the raised or
93 ombrotrophic bogs of the boreal zone are generally dominated by *Sphagnum* mosses that
94 contribute significantly to total ecosystem CO₂ flux (Oechel and Van Cleve, 1986;
95 Williams and Flanagan, 1998; Robroek et al., 2009; Vitt, 2014). *Sphagnum* mosses also
96 strongly affect the hydrological and hydrochemical conditions at the raised bog surface
97 (Van, 1995; Van der Schaaf, 2002). As a result, microclimate and *Sphagnum* species
98 interactions influence the variability of both carbon accumulation rates and water and
99 exchanges within peatland and between peatland and atmosphere (Heijmans et al., 2004a,
100 2004b; Rosenzweig et al., 2008; Brown et al., 2010; Petrone et al., 2011; Goetz and Price,
101 2015). Functioning as keystone species of boreal peatlands, *Sphagnum* mosses strongly
102 influence the nutrient, carbon and water cycles of peatland ecosystems (Nilsson and
103 Wardle, 2005; Cornelissen et al., 2007; Lindo and Gonzalez, 2010; Turetsky et al., 2010;
104 Turetsky et al., 2012), and exert a substantial impact on ecosystem net carbon balance
105 (Clymo and Hayward; 1982; Gorham, 1991; Wieder, 2006; Weston et el., 2015; Walker
106 et al., 2017; Griffiths et al., 2018).

107 Numerical models are useful tools to identify knowledge gaps, examine long-term
108 dynamics, and predict future changes. Earth system models (ESMs) simulate global
109 processes, including the carbon cycle, and are primarily used to make future climate
110 projections. Poor model representation of carbon processes in peatlands is identified as a

111 deficiency causing biases in simulated soil organic mass and heterotrophic respiratory
112 fluxes for current ESMs (Todd-Brown et al., 2013; Tian et al., 2015). Although most
113 ESMs do not include moss, a number of offline dynamic vegetation models and
114 ecosystem models do include one or more moss plant functional types (PFTs) (Pastor et
115 al., 2002; Nungesser, 2003; Zhuang et al., 2006; Bond-Lamberty et al., 2007; Heijmans et
116 al., 2008; Euskirchen et al., 2009; Wania et al., 2009; Frolking et al., 2010). Several
117 peatland-specific models contain moss species and have been applied globally or at
118 selected peatland sites. For example, the McGill Wetland Model (MWM) was evaluated
119 using the measurements at Degerö Stormyr and the Mer Bleue bogs (St-Hilaire et al.,
120 2010). The peatland version of the General Ecosystem Simulator - Model of Raw Humus,
121 Moder and Mull (GUESS-ROMUL) was used to simulate the changes of daily CO₂
122 exchange rates with water table position at a fen (Yurova et al., 2007). The PEATBOG
123 model was implemented to characterize peatland carbon and nitrogen cycles in the Mer
124 Bleue bog, including moss PFTs but without accounting for microtopography (Wu et al.,
125 2013a). The CLASS-CTEM model (the coupled Canadian Land Surface Scheme and the
126 Canadian Terrestrial Ecosystem Model), which includes a moss layer as the first soil
127 layer, was applied to simulate water, energy and carbon fluxes at eight different peatland
128 sites (Wu et al., 2016). The IAP-RAS (Institute of Applied Physics – Russian Academy
129 of Sciences) wetland methane (CH₄) model with a 10 cm thick moss layer (Mokhov et al.
130 2007) was run globally to simulate the distribution of CH₄ fluxes (Wania et al., 2013).
131 The CHANGE model (a coupled hydrological and biogeochemical process simulator),
132 which includes a moss cover layer (Launiainen et al., 2015), was used to investigate the
133 effect of moss on soil temperature and carbon flux at a tundra site in Northeastern Siberia

134 (Park et al., 2018). Chadburn et al. (2015) added a surface layer of moss to JULES land
135 surface model to consider the insulating effects and treated the thermal conductivity of
136 moss depending on its water content to investigate the permafrost dynamics. Porada et al.
137 (2016) integrated a stand-alone dynamic non-vascular vegetation model LiBry (Porada et
138 al., 2013) to land surface scheme JSBACH, but JSBACH mainly represent bryophyte and
139 lichen cover on upland forest, not for peatland ecosystem. Druel et al. (2017) investigated
140 the vegetation-climate feedbacks in high latitudes by introducing a non-vascular plant
141 type representing mosses and lichens to the global land surface model ORCHIDEE.
142 Moreover, those models did not consider microtopography and the lateral transports
143 between hummocks and hollows. Two models, the “ecosys” model (Grant et al., 2012)
144 and CLM_SPRUCE (Shi et al., 2015), have been parameterized to represent peatland
145 microtopographic variability (e.g., the hummock and hollow microterrain characteristic
146 of raised bogs) with lateral connections across the topography. Prediction of water table
147 dynamics in the “ecosys” model is constrained by specifying a regional water table at a
148 fixed height and a fixed distance from the site of interest, thereby missing key controlling
149 factors of a precipitation-driven dynamic water table (Shi et al., 2015). The
150 CLM_SPRUCE model (Shi et al., 2015) was developed to parameterize the hydrological
151 dynamics of lateral transport for microtopography of hummocks and hollows in the raised
152 bog environment of the SPRUCE (Spruce and Peatland Responses Under Changing
153 Environments) experiment (Hanson et al., 2017). That model version did not include the
154 biophysical dynamics of *Sphagnum* moss, and used a prescribed leaf area instead of
155 allowing leaf area to evolve prognostically.

Deleted: without including an organic soil layer

Deleted: F

158 In this study, we introduce a new *Sphagnum* moss PFT into the model, and migrate
159 the entire raised-bog capability into the new Energy Exascale Earth System Model
160 (E3SM), specifically into version 1 of the E3SM land model (ELM v1, Ricciuto et al.,
161 2018). The objectives of this study are to: 1) introduce a *Sphagnum* PFT to the ELM
162 model with additional *Sphagnum*-specific processes to better capture the peatland
163 ecosystem; and 2) apply the updated ELM to explore how an ombrotrophic, raised-dome
164 bog peatland ecosystem will respond to different scenarios of warming and elevated
165 atmospheric CO₂ concentration.

166 **2. Model description**

167 **2.1 Model provenance**

168 ELM v1 is the land component of E3SM v1, which is supported by the US
169 Department of Energy (DOE). Developed by multiple DOE laboratories, E3SM consists
170 of atmosphere, land, ocean, sea ice, and land ice components, linked through a coupler
171 that facilitates across-component communication (Golaz et al., 2019). ELM was
172 originally branched from the Community Land Model (CLM4.5, Oleson et al., 2013),
173 with new developments that include representation of coupled carbon, nitrogen, and
174 phosphorus controls on soil and vegetation processes, and new plant carbon and nutrient
175 storage pools (Ricciuto et al., 2018; Yang et al., 2019; Burrows et al., 2020). Inputs of
176 new mineral nitrogen of ELM are from atmospheric deposition and biological nitrogen
177 fixation. The fixation of new reactive nitrogen from atmospheric N₂ by soil
178 microorganisms is an important component of nitrogen budgets. ELM follows the
179 approach of Cleveland et al. (1999) that uses an empirical relationship of biological

180 nitrogen fixation as a function of net primary production to predict the nitrogen fixation.

181 The model version used in this study is designated ELM ~~SPRUCE~~, and includes the new
182 implementation of *Sphagnum* mosses as well as the hydrological dynamics of lateral
183 transport between hummock and hollow microtopographies. The implementation has
184 been parameterized based on observations from the S1-Bog in northern Minnesota, USA,
185 as described by Shi et al. (2015), with additional details provided below.

Deleted:

Formatted: Font: Italic

186 2.2 Non-vascular plants: *Sphagnum* mosses

187 To represent non-vascular plant the *Sphagnum* mosses, we modified the C3 arctic
188 grasses equations as follows. We considered *Sphagnum* biomass to be represented mainly
189 by leaf and stem carbon (only a very shallow root). In addition, we modified the vascular
190 C3 arctic grasses equations for photosynthesis and stomatal conductance (see the below
191 new model development), and the associated parameters as reported by Table 1-3. We
192 use the same framework as for C3 arctic grasses, but the Ball-Berry slope term is assumed
193 to be zero and the intercept term is the conductance term as a function of water content of
194 *Sphagnum* mosses. For all other processes like the evapo(transpi)ration and associated
195 parameters not described below, we used the C3 arctic grasses equations (reported by
196 Oleson et al., 2013). Drying impacts the conductance and affects evapo(transpi)ration of
197 the internal water. The *specific leaf area* (SLA) and leaf C:N ratio parameters are strong
198 controls on *the maximum rate of Rubisco carboxylase activity* (V_{cmax}), and therefore
199 overall productivity and *Sphagnum* moss *leaf area index* (LAI). The high sensitivities
200 occur because LAI is a strong control on evapo(transp)iration.

Formatted: Font: Italic

201 2.3 New model developments

202 2.3.1 Water content dynamics of *Sphagnum* mosses

204 The main sources for water content of *Sphagnum* mosses are passive capillary
205 water uptake from peat, and interception of atmospheric water on the capitulum (growing
206 tip of the moss) (Robroek et al. 2007). Capillary water uptake, the internal *Sphagnum*
207 moss water content, is modeled as functions of soil water content and evaporation losses.
208 Water intercepted on the *Sphagnum* moss capitulum is modeled as a function of moss
209 foliar biomass, current canopy water, water drip, and evaporation losses.

210 Since evaporation at the *Sphagnum* surface depends on atmospheric water vapor
211 deficit, moss-atmosphere conductance and available water pool which depends on
212 capillary wicking of water up to the surface. we developed a relationship between
213 measured soil water content at depth and surface *Sphagnum* water content. At SPRUCE,
214 the peat volumetric water content is measured at several depths using automated sensors
215 (model 10HS, Decagon Devices, Inc., Pullman, WA) calibrated for the site-specific upper
216 peat soil using mesocosms (reference Figure S1, Hanson et al. 2017). During those
217 calibrations, we periodically sampled the surface *Sphagnum* for gravimetric water content
218 and water potential using a dew point potentiometer (WP4, Decagon Devices, Inc.),
219 which also provided a surface soil water retention curve. The destructive sampling of
220 surface *Sphagnum* was primarily hummock species but did included some hollow
221 species. The automated measurements of peat water content at 10 cm depth were shown
222 to be a good indicator of surface *Sphagnum* water content (Fig. 1). Based on this
223 relationship, we model the water content of *Sphagnum* moss due to capillary rise
224 ($W_{internal}$) (g water /g dry moss) as:

$$225 \quad W_{internal} = 0.3933 + 7.6227 / (1 + \exp(-(Soil_{vol} - 0.1571))) / 0.018 \quad (1)$$

226 where $Soil_{vol}$ is the averaged volumetric soil water of modeled soil layers nearest the

Formatted: Font: Italic

227 10cm depth horizon (layers 3 and 4 in the ELM v1 vertical layering scheme).

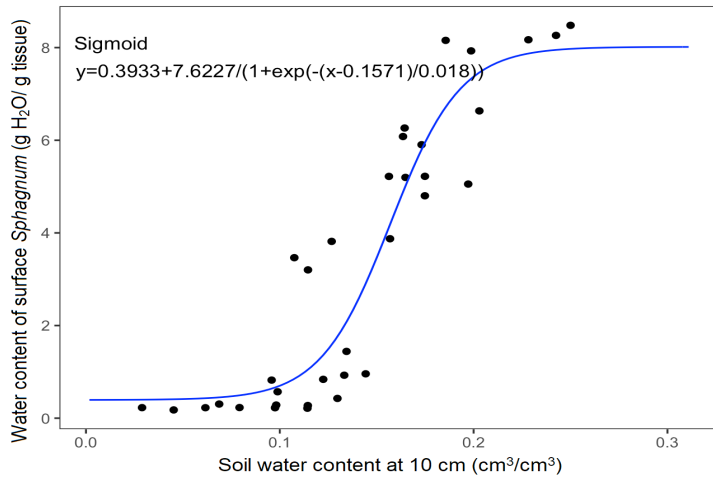
228 The *Sphagnum* moss surface water ($W_{surface}$) was calculated using the model
229 predicted canopy water and the dry foliar biomass as:

$$230 \quad W_{surface} = can_water / fmass \quad (2)$$

231 where $W_{surface}$ (g water /g dry moss) is the surface water content and $fmass$ is the foliar
232 biomass of *Sphagnum* mosses. The can_water is the *Sphagnum* moss canopy water and it
233 is simulated by a function of interception, canopy drip, dew and canopy evaporation
234 (Oleson et al., 2013).

235 The total water content (W_{total}) of *Sphagnum* mosses is the sum of water taken
236 up from peat and the surface water content (St-Hilaire et al, 2010; Wu et al., 2013).

$$237 \quad W_{total} = W_{internal} + W_{surface} \quad (3)$$



240 Figure 1. The measured relationship between soil water content at depth and the water content of
241 surface *Sphagnum* based on destructive sampling.

Formatted: Font: Italic

243 2.3.2 Modeling *Sphagnum* CO₂ conductance and photosynthesis

244 ELM_SPRUCE computes photosynthetic carbon uptake (gross primary
245 production, or GPP) for each vascular PFT on a half-hourly time step, based on the
246 Farquhar biochemical approach (Farquhar et al., 1980; Collatz et al., 1991, 1992), with
247 implementation as described by Oleson et al. (2013). While, *Sphagnum* lacks a leaf
248 cuticle and stomata that regulate water loss and CO₂ uptake in vascular plants (Titus et al.
249 1983). The primary transport pathway for CO₂ is through the cells and is analogous to
250 mesophyll conductance in higher plants. Thus, we calculate the total conductance to CO₂
251 for *Sphagnum* mosses by using total water content following the method reported by
252 Williams and Flanagan (1998) described as below. Goetz and Price (2015) also indicated
253 that capillary rise through the peat is essential to maintain a water content sufficient for
254 photosynthesis for *Sphagnum* moss species, but that atmospheric inputs can provide small
255 but critical amounts of water for physiological processes.

256 The stomatal conductance for vascular plant types in ELM_SPRUCE is derived
257 from the Ball-Berry conductance model (Collatz et al., 1991). That model relates
258 stomatal conductance to net leaf photosynthesis, scaled by the relative humidity and the
259 CO₂ concentration at the leaf surface. The stomatal conductance (g_s) and boundary layer
260 conductance (g_b) are required to obtain the internal leaf CO₂ partial pressure (C_i) of
261 vascular PFTs:

$$262 \quad C_i = C_a - \left(\frac{1.4g_s + 1.6g_b}{g_s g_b} \right) P_{atm} A_n \quad (4)$$

263 where C_i is the internal leaf CO₂ partial pressure, C_a is the atmospheric CO₂ partial
264 pressure, A_n is leaf net photosynthesis (μ mol CO₂ m⁻² s⁻¹) P_{atm} is the atmospheric
265 pressure, and values 1.4 and 1.6 are the ratios of the diffusivity of CO₂ to H₂O for
266 stomatal conductance and the leaf boundary layer conductance, respectively.

Deleted: g_s is the leaf stomatal conductance, g_b is the leaf boundary layer conductance,

267 For *Sphagnum* moss photosynthesis, we followed the method from the McGill
268 Wetland Model (St-Hilaire et al. 2010; Wu et al., 2013), which is based on the effects of
269 *Sphagnum* moss water content on photosynthetic capacity (Tenhunen et al., 1976) and
270 total conductance of CO₂ (Williams and Flanagan, 1998), and replaces the stomatal
271 conductance representation used for vascular PFTs.

$$272 \quad C_i = C_a - \frac{P_{atm} A_n}{g_{tc}} \quad (5)$$

273 The total conductance to CO₂ (g_{tc}) was determined from a least-squares regression
274 described by Williams and Flanagan (1998) as:

$$275 \quad g_{tc} = -0.195 + 0.134W_{total} - 0.0256W_{total}^2 + 0.0028W_{total}^3 - \\ 276 \quad 0.0000984W_{total}^4 + 0.00000168W_{total}^5 \quad (6)$$

277 where W_{total} is as defined in equation (3). This relationship is only valid up to the
278 maximum water holding capacity of mosses. To be noted that we assume that the
279 boundary layer conductance is greater than moss surface layer conductance, and the moss
280 surface layer conductance is greater than chloroplast conductance.

281 In addition to the water content, the effects of moss submergence were taken into
282 account in the calculation of moss photosynthesis. Walker et al. (2017) reported

285 significant impacts of submergence on measured *Sphagnum* GPP and modeled the effect
286 by modifying the *Sphagnum* leaf (stem) area index. Submergence in Walker et al. (2017)
287 was expressed as photosynthesising stem area index (SAI) as a logistic function of water
288 table depth. A maximum SAI of 3 was used and the parameter combination that most
289 closely described the GPP data gave a range of water table depth from -10 cm for
290 complete submergence and SAI of ~2.5 at 10 cm. This allowed for a range of processes
291 such as floatation of *Sphagnum* with the water table, and adhesion of water to the
292 *Sphagnum* capitula. For simplicity, in ELM_SPRUCE, we calculated such impacts on
293 *Sphagnum* GPP directly as a function of the height of simulated surface water, assuming
294 that GPP from the submerged portion of photosynthetic tissue is negligible. GPP is thus
295 reduced linearly according to the following equation:

$$296 \quad GPP_{\text{sub}} = GPP_{\text{orig}} * (h_{\text{moss}} - H_{2O_{\text{sfc}}}) \quad (7)$$

297 where GPP_{sub} is the GPP corrected for submergence effects, GPP_{orig} is the original GPP,
298 $H_{2O_{\text{sfc}}}$ is the surface water height, and h_{moss} is the height of the photosynthesizing
299 *Sphagnum* layer above the soil surface, set to 5cm in our simulations. If $H_{2O_{\text{sfc}}}$ is equal to
300 or greater than h_{moss} , GPP is reduced to zero. Because in our simulations surface water is
301 never predicted to occur in the hummocks, in practice this submergence effect only
302 affects the moss GPP in the hollows.

303 3. Methods

304 3.1 Site Description

305 We focused on a high C, ombrotrophic peatland (the S1-Bog) that has a perched
306 water table with limited groundwater influence (Sebestyen et al. 2011, Griffiths and

Formatted: Font: Italic

Formatted: Font: Italic

307 Sebestyen, 2016). This southern boreal bog is located on the Marcell Experimental
308 Forest, approximately 40 km north of Grand Rapids, Minnesota, USA (47.50283 degrees
309 latitude, -93.48283 degrees longitude) (Sebestyen et al. 2011), and is the site of the
310 SPRUCE climate change experiment (<http://mnspruce.ornl.gov>; Hanson et al., 2017). The
311 S1-Bog has a raised hummock and sunken hollow microtopography, and it is nearly
312 covered by *Sphagnum* mosses. *S. angustifolium* (C.E.O. Jensen ex Russow) and *S. fallax*
313 (Klinggr.) occupy 68% of the moss layer and exist in both hummocks and hollows. *S.*
314 *magellanicum* (Brid.) occupies ~20% of the moss layer and is primarily limited to the
315 hummocks (Norby et al., 2019). The vascular plant community at the S1-Bog is
316 dominated by the evergreen tree *Picea mariana* (Mill.) B.S.P, the deciduous tree *Larix*
317 *laricina* (Du Roi) K. Koch, and a variety of ericaceous shrubs. Trees are present due to
318 natural regeneration following strip cut harvesting in 1969 and 1974 (Sebestyen et al.,
319 2011). The soil of this peat bog is the Greenwood series, a Typic Haplohemist
320 (<https://websoilsurvey.sc.egov.usda.gov>), and its average peat depth is 2 to 3 m
321 (Parsekian et al., 2012)

322 Northern Minnesota has a subhumid continental climate with average annual
323 precipitation of 768 mm and annual air temperature of 3.3 °C for the time period from
324 1965 to 2005. Mean annual air temperatures at the bog have increased about 0.4 °C per
325 decade over the last 40 years (Verry et al., 2011).

326 **3.2 Field measurements**

327 Multiple observational pre-treatment data (the data were collected prior to
328 initiation of the warming and CO₂ treatments) were used in this study. Flux-partitioned
329 GPP of *Sphagnum* mosses was derived from measured hourly *Sphagnum*-peat net

330 ecosystem exchange (NEE) flux (Walker et al., 2017). The GPP – NEE relationship was
331 also evaluated using observed vegetation growth and productivity allometric and biomass
332 data on tree species, stem biomass for shrub species (Hanson et al., 2018a and b), and
333 *Sphagnum* pre-treatment net primary productivity (NPP) (Norby et al., 2019).
334 ELM_SPRUCE was driven by climate data (temperature, precipitation, relative humidity,
335 solar radiation, wind speed, pressure and long wave radiation) from 2011 to 2017
336 measured at the SPRUCE S1-Bog (Hanson et al., 2015a and b). The surface weather
337 station is outside of the enclosures and not impacted by the experimental warming
338 treatments that began in 2015. These data are available at <https://mnspruce.ornl.gov/>.

339 340 **3.3 Simulation of the SPRUCE experiment**

341 Based on measurements at the SPRUCE site, ELM_SPRUCE includes four
342 PFTs: boreal evergreen needleleaf tree (*Picea*), boreal deciduous needleleaf tree (*Larix*),
343 boreal deciduous shrub (representing several shrub species), and the newly introduced
344 *Sphagnum* moss PFT. Currently ELM_SPRUCE does not include light competition
345 among multiple PFTs, and thus does not represent cross-PFT shading effects. Our model
346 also allows the canopy density of PFTs to change prognostically, and their fractional
347 coverage is held constant. We used measurements from *Sphagnum* moss collected at a
348 tussock tundra site in Alaska (Hobbie 1996) to set several of the model leaf litter
349 parameters for our simulations (Table 1). The values for other parameters have been
350 optimized based on observations at the SPRUCE site (Table 2 and 3, optimization
351 methods described in section 3.4). We prescribe both hummock and hollow
352 microtopographies to have the same fractional PFT distribution. Consistent with Shi et

Deleted: <https://scratch.mit.edu/projects/411435898>

354 al. (2015), hummocks and hollows were modeled on separate columns with lateral flow
355 of water between them. All the ELM_SPRUCE simulations were conducted using a
356 prognostic scheme for canopy phenology (Olesen et al., 2013).

357 The SPRUCE experiment at the S1-Bog consists of combined manipulations of
358 temperature (various differentials up to +9 °C above ambient) and atmospheric CO₂
359 concentration (ambient and ambient + 500 ppm) applied in 12 m diameter x 8 m tall
360 enclosures constructed in the S1-Bog. The whole-ecosystem warming began in August
361 2015, elevated CO₂ started from June 2016, and various treatments are envisioned to
362 continue until 2025. Extensive pre-treatment observations at the site began in 2009.

363 For the ELM_SPRUCE, we continuously cycled the 2011-2017 climate forcing
364 (see section 3.2) to equilibrate carbon and nitrogen pools under pre-industrial
365 atmospheric CO₂ concentrations and nitrogen deposition, and then launched a simulation
366 starting from year 1850 through year 2017. This transient simulation includes historically
367 varying CO₂ concentrations, nitrogen deposition, and the land-use effects of a strip cut
368 and harvest at the site in 1974. These simulations were used to compare model
369 performance with pre-treatment observations. A subset of these observations was also
370 used for optimization and calibration (section 3.4).

371 To investigate how the bog vegetation may respond to different warming
372 scenarios and elevated atmospheric CO₂ concentrations, we performed 11 model runs
373 from the same starting point in year 2015. These simulations were designed to reflect the
374 warming treatments and CO₂ concentrations being implemented in the SPRUCE
375 experiment enclosures. The model simulations include one ambient case (both ambient
376 temperature and CO₂ concentration), and five simulations with modified input air

377 temperatures to represent the whole-ecosystem warming treatments at five levels (+0 °C,
 378 +2.25 °C, +4.50 °C, +6.75 °C and +9.00 °C above ambient) and at ambient CO₂, and
 379 another five simulations with the same increasing temperature levels and at elevated CO₂
 380 (900 ppm). In the treatment simulations, we also considered the passive enclosure
 381 effects, which reduce incoming shortwave and increase incoming longwave radiation
 382 (Hanson et al., 2017). Following the SPRUCE experimental design, there was no water
 383 vapor added so that the simulations used constant specific humidity instead of constant
 384 relative humidity across the warming levels. All the treatment simulations were
 385 performed through the year 2025 by continuing to cycle the 2011-2017 meteorological
 386 inputs (with modified temperature and radiation to reflect the treatments) to simulate
 387 future years.

388 Table 1: Physiological parameters of *Sphagnum* mosses as given in Hobbie 1996

Parameters	Description	Values
lfliten	Leaf litter C:N ratio (gC/gN)	66
lf_fcel	Leaf litter fraction of cellulose	0.737
lf_flab	Leaf litter fraction of labile	0.227
lf_flg	Leaf litter fraction of lignin	0.036

389

390 **3.4. Model sensitivity analysis and calibration**

391 The vegetation physiology parameters in ELM_SPRUCE were originally derived
 392 from CLM4.5 and its predecessor, Biome-BGC, and represent broad aggregations of
 393 plant traits over many species and varied environmental conditions (White et al., 2000).

394 To achieve reasonable model performance at SPRUCE, site-specific parameters and
395 targeted parameter calibration are needed. Since the ELM_SPRUCE contains over 100
396 uncertain parameters, parameter optimization is not computationally feasible without first
397 performing some dimensionality reduction. Based on previous ELM sensitivity analyses
398 (e.g., Lu et al., 2018; Ricciuto et al., 2018; Griffiths et al., 2018), we chose 35 model
399 parameters for further calibration (Tables 2 and 3). An ensemble of 3000 ELM_SPRUCE
400 simulations were conducted using the procedure described in 3.3, with each ensemble
401 member using a randomly selected set of parameter values within uniform prior ranges.
402 This model ensemble was first used to construct a polynomial chaos surrogate model,
403 which was then used to perform a global sensitivity analysis (Sargsyan et al., 2014;
404 Ricciuto et al., 2018). Main sensitivity indices, reflecting the proportion of output
405 variance that occurs for each parameter, are described in section 4.1.

406 To minimize potential biases in model predictions of treatment responses, we
407 calibrated the same 35 model parameters using pre-treatment observations as data
408 constraints. We employed a quantum particle swarm optimization (QPSO) algorithm (Lu
409 et al., 2018). While this method does not allow for the calculation of posterior prediction
410 uncertainties, it is much more computationally efficient than other methods such as
411 Markov Chain Monte Carlo. The constraining data included year 2012-2013 tree growth
412 and biomass (Hanson et al. 2018a), year 2012-2013 shrub growth and biomass (Hanson
413 et al., 2018b), year 2012 and 2014 *Sphagnum* net primary productivity (Norby et al.,
414 2017, 2019), enclosure-averaged leaf area index by PFT (year 2011 for tree and year
415 2012 for shrub and *Sphagnum*), and year 2011-2013 water table depth (WTD)
416 observations, aggregated to seasonal averages (Hanson et al., 2015b). The goal of the

417 optimization is to minimize a cost function, which we define here as a sum of squared
 418 errors over all observation types weighted by observation uncertainties. When
 419 observation uncertainties were not available, we assumed a range of $\pm 25\%$ from the
 420 default value. Site measurements were also used to constrain the ranges of two
 421 parameters: *leafcn* (leaf carbon to nitrogen ratio) and *slatop* (specific leaf area at canopy
 422 top). The uniform prior ranges for these parameters represent the range of plot to plot
 423 variability. Optimized parameter values are shown in Table 2 and 3. Section 4 reports the
 424 results of simulations using these optimized parameters, which were used to perform a
 425 spinup, transient (1850-2017) and set of 11 treatment simulations (2015-2025) as
 426 described above.

427 Table 2: PFT-specific optimized model parameters

Parameter	Description	<i>Sphagnum</i>	<i>Picea</i>	<i>Larix</i>	Shrub	Range
flnr	Rubisco-N fraction of leaf N	0.2906	0.0678	0.2349	0.2123	[0.05,0.30]
croot_stem	Coarse root to stem allocation ratio	N/A	0.2540	0.1529	0.7540	[0.05,0.8]
stem_leaf ¹	Stem to leaf allocation ratio	N/A	1.047	1.016	0.754	[0.3,2.2]
leaf_long	Leaf longevity (yr)	0.9744	5 ³	N/A	N/A	[0.75, 2.0]
slatop	Specific leaf area at canopy top (m ² gC ⁻¹)	0.00781	0.00462	0.0128	0.0126	[0.004,0.04]
leafcn	Leaf C to N ratio	35.56	70.17	64.84	33.14	[20,75]
froot_leaf ²	Fine root to leaf allocation ratio	0.3944	0.8567	0.3211	0.6862	[0.15, 2.0]
mp	Ball-Berry stomatal conductance slope	N/A	7.50	9.32	10.8	[4.5, 12]

428 Optimized values of PFT-specific parameters. The range column values in brackets indicate the range of
 429 acceptable parameter values used in the sensitivity analysis and the optimization across all four PFTs in the
 430 format [minimum, maximum]. N/A indicates that parameter is not relevant for that PFT.

431 ¹for tree PFTs, this parameter depends on NPP. The value shown is the allocation at an NPP of 800 gC m⁻²
 432 yr⁻¹.

433 ² the fine root pool is used as a surrogate for non-photosynthetic tissue in *Sphagnum*

434 ³ This parameter was not optimized; we used the default value.

435

436

437 Table 3: Non PFT-specific optimized model parameters

	Description	Optimized value	Default	Range
r_mort	Vegetation mortality	0.0497	0.02	[0.005, 0.1]
dcomp_depth_efolding	Depth-dependence e-folding depth for decomposition (m)	0.3899	0.5	[0.2, 0.7]
Q _{drai,0}	Maximum subsurface drainage rate (kg m ⁻² s ⁻¹)	3.896e-6	9.2e-6*	[0, 1e-3]
Q _{10_mr}	Temperature sensitivity of maintenance respiration	2.212	1.5	[1.2, 3.0]
br_mr	Base rate for maintenance respiration (gC gN m ² s ⁻¹)	4.110e-6	2.52e-6	[1e-6, 5e-6]
crit_onset_gdd	Critical growing degree days for leaf onset	99.43	200	[20, 500]
lw_top_ann	Live wood turnover proportion (yr ⁻¹)	0.3517	0.7	[0.2, 0.85]
gr_perc	Growth respiration fraction	0.1652	0.3	[0.12, 0.4]
Γ _{drai,0}	Coefficient for surface water runoff (kg m ⁻⁴ s ⁻¹)	6.978e-7	8.4e-8*	[1e-9, 1e-6]

438 Optimized and default values for non PFT-specific parameters. The range column values in brackets
 439 indicate the range of acceptable parameter values used in the sensitivity analysis and the
 440 optimization in the format [minimum, maximum].
 441 * Previously calibrated value from Shi et al (2015)

442

443 4. Results

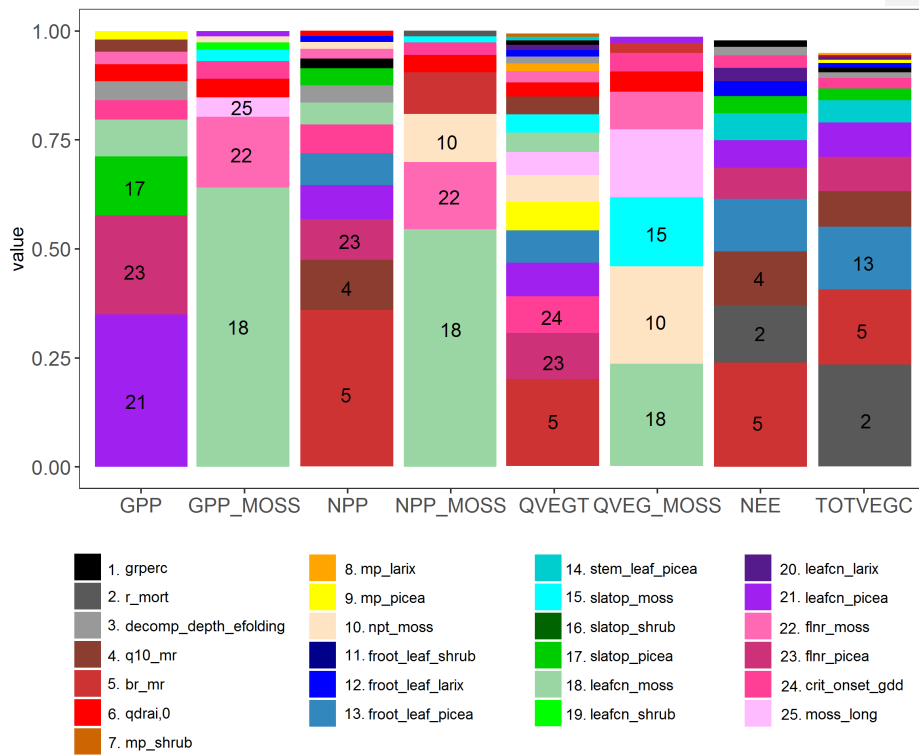
444 4.1 Model sensitivity analysis

445 Main effect (first-order) sensitivities are shown for eight model output quantities of
 446 interest: Total site gross primary productivity (GPP), GPP for the moss PFT only
 447 (GPP_moss), total site net primary productivity (NPP), NPP for the moss PFT only
 448 (NPP_moss), total site vegetation transpiration (QVEGT), evaporation from the moss
 449 surface (QVEG_moss), net ecosystem exchange (NEE) and site total vegetation carbon

450 (TOTVEGC) (Fig. 2). Out of 35 parameters investigated, 25 show a sensitivity index of
451 at least 0.01 for one of the quantities of interest, and these are plotted on figure 2. In that
452 figure, sensitivities are stacked in order from highest to lowest for each variable, with the
453 height of the bar equal to the sensitivity index. The first order sensitivities sum to at least
454 0.95 for all variables, indicating that higher order sensitivities (i.e., contributions to the
455 sensitivity from combinations of two or more parameters) contribute relatively little to
456 the variance for these quantities of interest.

457 According to this analysis, the variance in total site GPP is dominated by three
458 *Picea* parameters: the fraction of leaf nitrogen in RuBiCO (*flnr_picea*), leaf carbon to
459 nitrogen ratio (*leafcn_picea*) and the specific leaf area at canopy top (*slatop_picea*). GPP
460 sensitivity for the moss PFT is dominated by the same three parameters, but for the moss
461 PFT instead of *Picea* (*flnr_moss*, *leafcn_moss*, and *slatop_moss*). For NPP, QVEGT and
462 NEE, the highest sensitivity the maintenance respiration base rate *br_mr*, similar to
463 earlier results in Griffiths et al. (2017). The maintenance respiration temperature
464 sensitivity Q_{10_mr} is also a key parameter for NPP and NEE. The critical onset growing
465 degree day threshold (*crit_onset_gdd*), which drives deciduous phenology in the spring
466 for the *Larix* and shrub PFTs, is an important parameter for NPP and NEE. *flnr_picea* is
467 important for both NPP and QVEGT. For NPP_moss and QVEG_moss, *leafcn_moss* is
468 and the ratio of non-photosynthesizing tissue to photosynthesizing tissue (*npt_moss*) are
469 sensitive. For TOTVEGC and NEE, vegetation mortality (*r_mort*) is also a sensitive
470 parameter. For the site-level quantities of interest, at least 10 parameters contribute
471 significantly to the uncertainty, illustrating the complexity of the model and large number
472 of processes contributing to uncertainty in SPRUCE predictions. For the moss variables,

473 there are some cases where significant sensitivities exist for non-moss PFT parameters.
 474 For example, *leafcn_shrub* is the seventh most sensitive parameter for GPP_moss,
 475 indicating that competition between the PFTs for resources may be important. In this
 476 case, uncertainty about parameters on one PFT may drive uncertainties in the simulated
 477 productivity of other PFTs.



478

479 Figure 2 Sensitivity analysis of ELM-SPRUCE for selected parameters (Table 2 and 3). The
 480 Colored bars indicate the fraction of variance in site gross primary productivity (GPP), moss-only
 481 NPP (GPP_MOSS), site net primary productivity (NPP), moss-only NPP (NPP_MOSS), total
 482 vegetation transpiration (QVEGT), moss evaporation (QVEG_MOSS), site net ecosystem
 483 exchange (NEE) and total vegetation carbon (TOTVEGC) controlled by each parameter. The
 484 legend shows the top 25 most influential parameters; the remaining parameters not shown have
 485 sensitivities of no more than 0.01 for any of the outputs. All variables represent 2011-2017

486 average values over the ambient conditions. For parameters that are treated as PFT-dependent,
487 the PFT is indicated with a suffix (picea, larix, shrub or moss)
488

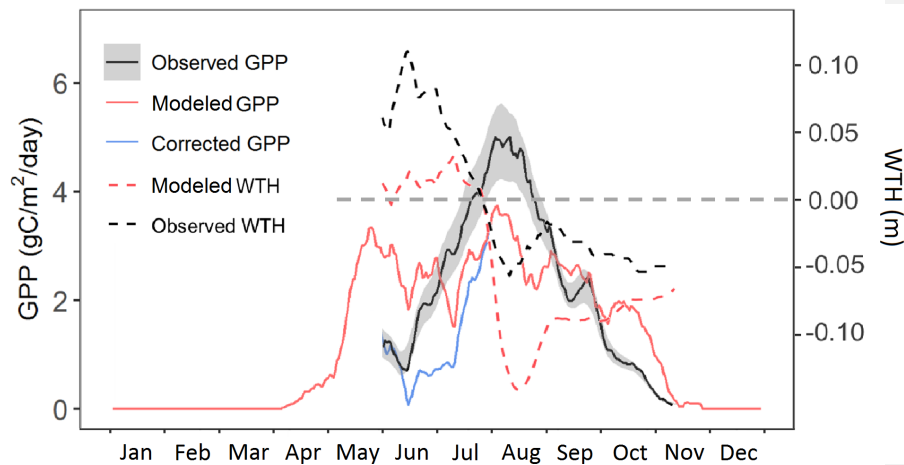
489 **4.2 Model evaluation**

490 Our model simulates GPP for vascular plants and *Sphagnum* moss in both
491 hummock and hollow settings, with separate calculations for each PFT. Here we use the
492 model estimate of GPP prior to downregulation by nutrient limitation from the ambient
493 case, based on recent studies indicating that nutrient limitation effects are occurring
494 downstream of GPP (Raczka et al. 2016; Metcalfe et al., 2017; Duarte et al. 2017). This
495 treatment of nutrient limitation on GPP has been modified in a more recent version of
496 ELM, and our moss modifications will be merged to that version as a next step. For now,
497 by referring to the pre-downregulation GPP we are capturing the most significant impact
498 of those changes for the purpose of comparison to observations.

499 Our model simulated two seasonal maxima of *Sphagnum* moss GPP, one at the
500 end of May, and the other in August (Figure 3). Both peaks are lower than the maximum
501 of observed (flux-partitioned) GPP, which occurs in August. Based on results of the
502 sensitivity analysis, it could be that the base rate for maintenance respiration for moss is
503 too high, causing an underestimate of NPP and biomass, which leads to a low bias in
504 peak GPP.

505 During June and October, observations suggest that ELM_SPRUCE over-predicts
506 GPP. The model does limit GPP as a function of the depth of standing water on the bog
507 surface (Eq. 7). The water table height (WTH) above the bog surface is being predicted
508 by the model (dashed red line in Fig. 3), and while the seasonal pattern of higher water

509 table in the spring and lower water table in the fall agrees well with observations (dashed
 510 black line in Fig. 3), the predicted WTH is generally too low by 5-10 cm. The modeled
 511 WTH here is for hollow. We turned off the lateral transport when there is ice on the soil
 512 layers above the water table to avoid an unreasonable amount of ice accumulation on the
 513 frozen layers, which results in there is no flow from hummock to hollow. Forcing the
 514 modeled GPP to respond to observed WTH (during the period with observations) gives a
 515 pattern of increasing GPP through June and July which is more consistent with
 516 observations (blue line in Fig. 3). We do not have observations for GPP earlier than June,
 517 due to limitations of the instrumentation when the bog surface is flooded.

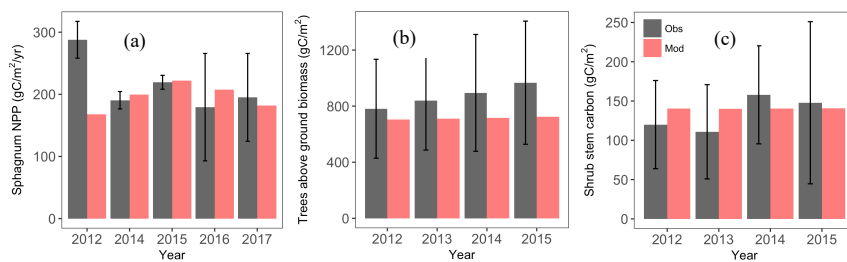


518
 519
 520 Figure 3. Predicted GPP (red solid line) compared with flux-partitioned GPP (black solid line,
 521 GPP data was not used in the parameters optimization) of *Sphagnum* mosses for the year 2014.
 522 The blue line is the predicted GPP corrected with the observed water table height. The dashed
 523 black and red lines are observed and modeled water table height (the dashed gray line is the
 524 hollow surface).

525
 526
 527 The model simulated reasonable annual values for *Sphagnum* NPP for the period
 528 2014-2017 but showed much lower NPP compared with observation (139 vs. 288 g

529 $C/m^2/yr$) for the year 2012 (Fig. 4a). Measurement uncertainties are larger in 2016-2017
 530 than in earlier years, perhaps related to a new measurement protocol for those years, and
 531 the model estimates are within measurement uncertainty bounds for years 2014-2017
 532 (Griffiths et al., 2018; Norby et al., 2019). The observed *Sphagnum* NPP was measured at
 533 different plots and each plot included different species abundances. As a result, the scaled
 534 NPP includes spatial variations and uncertainty in species distribution (Norby and Childs,
 535 2017).

536 Simulated tree above ground biomass is within the observed inter-plot variability
 537 (Fig. 4b). Observations suggest an increasing trend in tree biomass, which was not
 538 predicted by the model. The optimized parameters show increased mortality and
 539 autotrophic respiration rate parameters compared to the default model (Table 3), which
 540 causes the simulations to approach steady state relatively quickly after the 1974
 541 disturbance. However, the sensitivity analysis also identifies these mortality and
 542 maintenance respiration parameters as highly sensitive, therefore this simulated response
 543 is uncertain. For the shrub stem carbon, the simulated mean from year 2012 to 2015 was
 544 $140.4 g C/m^2$, slightly higher than the observation ($133.9 g C/m^2$) but well within the
 545 observed range of inter-plot variability (Fig. 4c).



546

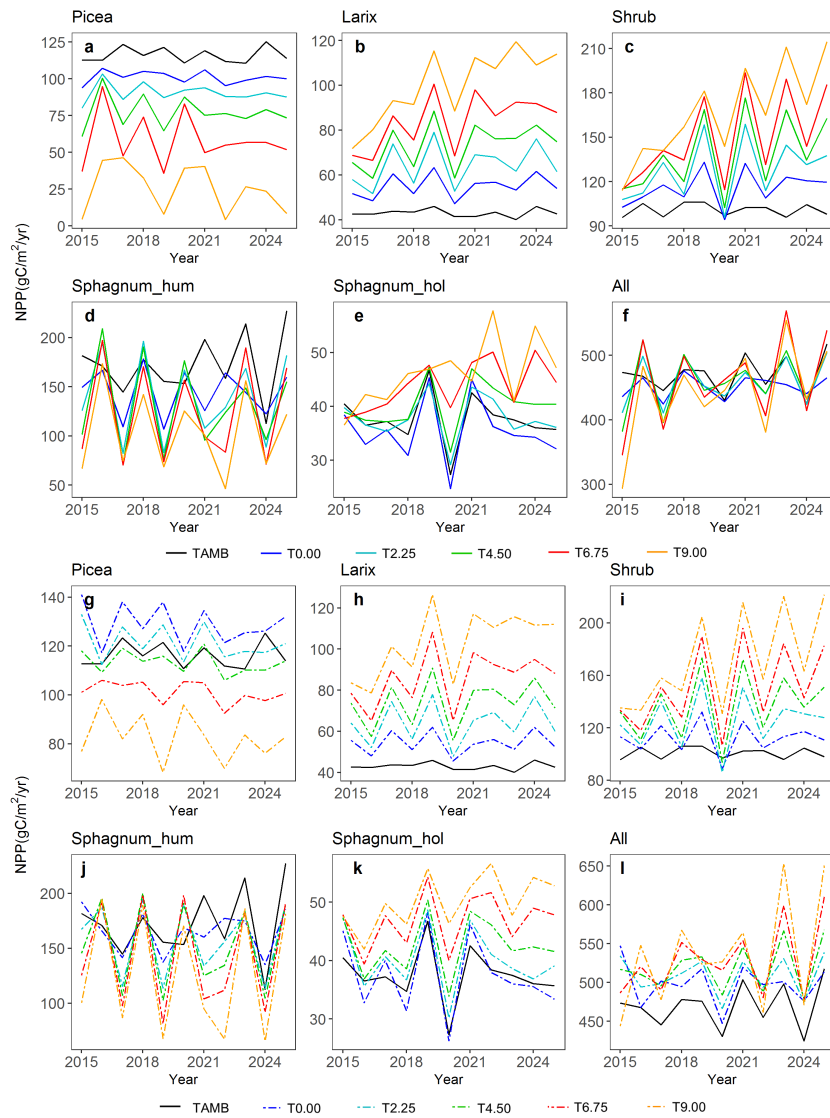
547 Figure 4. Predicted (red bars) *Sphagnum* NPP (left), aboveground tree biomass (middle) and
548 shrub stem carbon (right) compared with the observations (black bars). Observed NPP data are
549 based on growth of 12-17 bundles of 10 *Sphagnum* stems in 2012-2015 (unpublished data) and
550 in two ambient plots by the method described by Norby et al. (2019) in 2016-2017 (data in
551 Norby et al. 2017). The *Sphagnum* NPP data of year 2015-2017, and aboveground tree biomass
552 and shrub stem carbon of year 2014-2015 are independent of the related parameters
553 optimization.

Formatted: Font: Italic

555 4.3 Simulated carbon cycle response to warming and elevated atmospheric CO₂ 556 concentration

557 Different PFTs demonstrated different warming responses for both ambient CO₂
558 and elevated CO₂ concentration conditions (Fig. 5). Both *Larix* and shrub NPP increased
559 with warming under both CO₂ concentration conditions (Fig. 5 b, c, h and i). In addition,
560 CO₂ fertilization stimulates the growth of these two PFTs and the fertilization effect
561 further increases with warming (Fig. S1). In contrast, *Picea* NPP decreased with warming
562 levels (Fig. 5 a and g) for both CO₂ conditions. For *Sphagnum*, NPP decreased in
563 hummocks but increased in hollows with increasing temperature (Fig. 5 d, e, j and k).
564 The CO₂ fertilization also stimulate the grow of the *Picea* and *Sphagnum* PFTs (Fig. 5 a,
565 d, e g, j and k). The enclosure-total NPP for all PFTs responded differently to the
566 warming only and warming with elevated CO₂ (Fig. 5 f and l). The enclosure-total NPP
567 for each warming level changed less under the ambient CO₂ condition than those with
568 elevated CO₂ condition, and NPP decreased with warming in most of years under
569 ambient CO₂ condition but increased under elevated CO₂ condition (Fig.5 f and l). This
570 result demonstrated that the elevated CO₂ scenario changes the sign of the NPP warming
571 response for the bog peatland ecosystem.

Deleted: , GPP increases more under elevated CO₂ condition than the ambient case



574
 575 Figure 5 predicted NPP response to warming with ambient atmospheric CO₂ (a-f, solid lines) and
 576 warming with elevated atmospheric CO₂ concentration (g-l, dash lines), the black solid line
 577 TAMB is the ambient temperature and CO₂ case, T0.00 to T9.00 means increasing temperature
 578 from 0°C to 9°C
 579

580 Compared with the ambient biomass, the biomass of black spruce (*Picea*)
581 significantly decreased but the biomass of *Larix* significantly increased under the greatest
582 warming treatment (+9.00°C, Fig.6). Biomass of shrub and hollow *Sphagnum* also
583 increased, but less than did *Larix*. The hummock *Sphagnum* biomass also showed strong
584 correlation with water table height at roughly a 3-month lag (the maximum correlation
585 occurs with an 82-day lag, $R^2=0.56$). NPP is allocated instantaneously into biomass. A
586 positive NPP anomaly caused by water table shifts leads to higher LAI, which also
587 increases future productivity for some amount of time even if the water table returns to
588 normal. *Sphagnum* biomass has a 1-year turnover time in the simulation. This
589 combination of effects leads to a roughly 3-month timelag. Due to the relative lower
590 height of the water table in the hummock than the hollow, the simulated hummock
591 *Sphagnum* were more significantly water-stressed than the hollow *Sphagnum* as the water
592 table height declines. This is consistent with multiple studies finding an increase in
593 temperatures associated with drought (low water table height) reducing *Sphagnum*
594 growth (Bragazza et al., 2016; Granath et al., 2016; Mazziotta et al., 2018). We plotted
595 the predicted canopy evaporation for hummock and hollow *Sphagnum* responses to
596 warming and found that both hummock and hollow *Sphagnum* canopy evaporation
597 increase with warming for both ambient and elevated atmospheric CO₂ conditions despite
598 the *Larix* and shrubs are growing with warming. Moreover, the hollow *Sphagnum* canopy
599 evaporation warming response is stronger than that of the hummock *Sphagnum* (Fig. S2).
600 In summary, the growth of bog vegetation is predicted to have species-specific warming
601 responses that differ in sign and magnitude.

Formatted: Font: Italic

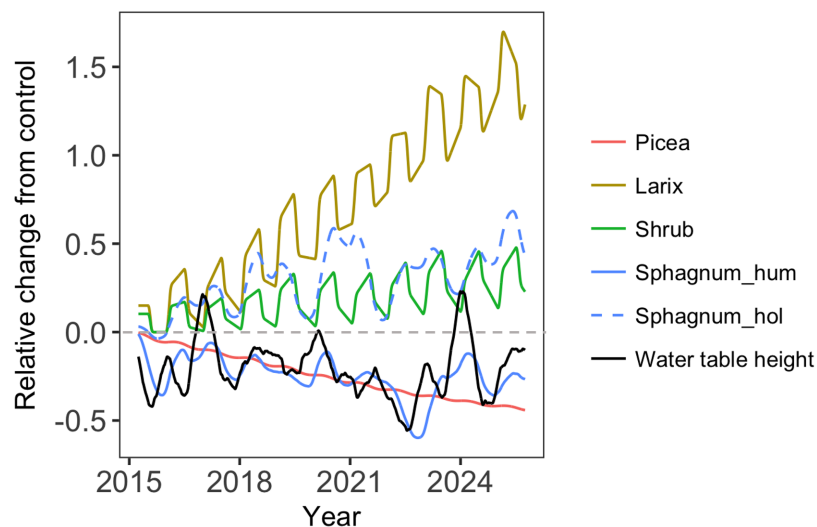
Formatted: Font: Italic

Formatted: Font: Italic

Formatted: Subscript

Formatted: Font: Italic

Formatted: Font: Italic



602
 603 Figure 6 The relative changes of biomass for different PFTs and water table height (the weighted
 604 average between hummock and hollow) between +9.00 °C treatment case and the ambient case
 605 (+9.00 °C / ambient – 1)

606 **5. Discussion**

607 *Sphagnum* moss is the principal plant involved in the peat accumulation in peatland
 608 ecosystems, and effective characterization of its biophysical and physiological responses
 609 has implications for predicting peatland and global carbon, water and climate feedbacks.
 610 This study moves us closer to our long-term goal of improving the prediction of peatland
 611 water, carbon and nutrient cycles in ELM_SPRUCE, by introducing a new *Sphagnum*
 612 moss PFT, implementing water content dynamics and photosynthetic processes for this
 613 nonvascular plant. The *Sphagnum* model development combined with our previous
 614 hummock-hollow microtopography representation and laterally-coupled two-column
 615 hydrology scheme enhance the capability of ELM_SPRUCE in simulating high-carbon
 616 wetland hydrology and carbon interactions and their responses to plausible environmental
 617 changes.
 618

619
620 **5.1 Uncertainties in simulating *Sphagnum* productivity**

621 Our predicted peak GPP is similar to the results found by Walker et al. (2017)
622 when they calculated the internal resistance to CO₂ diffusion as a function of *Sphagnum*
623 water content using a stand-alone photosynthesis model. In both cases, the predicted peak
624 GPP is lower than observations. Walker et al. (2017) were, however, able to capture the
625 observed peak magnitude with a combination of light extinction coefficient, canopy
626 clumping coefficient, maximum SAI, and a logistic function describing the effective
627 *Sphagnum* SAI in relation to water table. Here we used model default values for the light
628 extinction and canopy clumping coefficients. While the water table impacts *Sphagnum*
629 productivity in our simulation, modeled LAI is mainly controlled by NPP and turnover.
630 In addition, we use the default formulation for acclimation of V_{cmax} in ELM which is
631 based on a 10-day mean growing temperature. At this point we don't have sufficient
632 measurements to test this assumption, but we can prioritize these measurements in the
633 future. *Sphagnum* temperature is computed from surface energy balance but because the
634 current model doesn't estimate the shading effects from trees and shrubs, this may be
635 overestimated. Moreover, biases in predicted water table height contribute to errors in
636 the calculated submergence effect. Improving these biases and assuming an exponential
637 rather than a linear CO₂ uptake profile may improve representation of the submergence
638 effect. All these aspects may be attribute to the biases of the simulated *Sphagnum* GPP.
639 We can consider this in the future when we have more detailed measurements. Further
640 investigation is thus needed to understand how representative the chamber-based
641 observations from Walker et al. (2017) are of the larger-scale SPRUCE enclosures, and to
642 reconcile these GPP estimates with plot-level NPP observations (Norby et al., 2019).

Deleted: shoot area index (

Deleted:)

Deleted: leaf (or shoot) area index (

Deleted:)

Deleted: have the capacity to

Formatted: Subscript

Formatted: Font: Italic

648 The hydrology cycle, especially water table depth (WTD) is also a key factor that
649 influences the seasonality of GPP in *Sphagnum* mosses (Lafleur et al., 2005; Riutta 2007,
650 Sonntag et al, 2010; Grant et al., 2012; Kuiper et al., 2014; Walker et al, 2017). One
651 key feedback is if the water table declines, there can be enhanced decomposition and
652 subsidence of the peat layer, which brings the surface down closer to the water table
653 again. But we currently did not consider the peat layer elevation changes in our model
654 and this will be one of the future development directions. The capillary rise plays into the
655 *Sphagnum* hydrological balance, which varies depending on water table depth and
656 evaporative demand. At short timescales or under rapidly changing conditions, there may
657 not be equilibration between the *Sphagnum* water content and the peat moisture.
658 Generally, the *Sphagnum* water content will equilibrate with the peat on a daily basis
659 outside the plot since the dew point is often reached at night. But since the vapor pressure
660 deficit does not go to zero inside the warmer plots, some disequilibration could remain.
661 High-frequency latent heat flux data from the site are currently lacking, but could help to
662 constrain these effects in the future.

663 ____ The current phenology observations also include if *Sphagnum* hummock and hollow
664 are wet or dry, and we could look at the relationship with soil water content sensors in the
665 future. Moreover, the timescales for rewetting may change as the peat dries since the
666 cross section for capillary rise will decline and thus the maximum flux to the surface will
667 decline. At some point, between gravity potential and reduced hydraulic conductivity, we
668 expect that the capillarity will no longer satisfy evaporative demand. Alternately, under
669 saturated conditions when the water table is close to the *Sphagnum* surface, *Sphagnum*
670 photosynthesizing tissue can become submerged or surrounded by a film of water that is

- Formatted: Font: Italic
- Formatted: Font: Italic
- Deleted: s
- Formatted: Font: Italic
- Formatted: Font: Italic
- Deleted: the equilibration time between peat moisture and moss water content is reasonable fast, but the
- Deleted: should
- Deleted: So,
- Deleted: a
- Deleted: not
- Deleted: (Personal discussion with field expert Jeffrey Warren)
- Deleted: Previous studies have reported that drier and warmer future climates can lower the water table, affecting the resilience of long-term boreal peatland carbon stocks (Limpens et al., 2008, Dise, 2009, Frohling et al., 2011). WTD drawdown affects the net ecosystem productivity of boreal peatlands through its effects on ecosystem respiration and GPP. The interactions between WTD and GPP, however, vary across peatlands and influence both vascular and nonvascular plant GPP in different ways (Lafleur et al., 2005). For instance, nonvascular plants mostly access water in the near surface shallow peat layers. These layers, however, can drain quickly with receding WTD and high nonvascular evaporative demand, and thus depend on water supply through capillary rise or precipitation (Dimitrov et al., 2011, Peichl et al., 2014, Druel et al., 2017). If recharge is not adequate, near-surface peat desiccation occurs thereby cutting off the supply of water to *Sphagnum*, which subsequently dries, leading to rapid decline in GPP (Lafleur et al., 2005, Riutta 2008, Sonntag et al., 2010, Sulman et al., 2010, Dimitrov et al., 2011, Kuiper et al., 2014, Peichl et al., 2014). Thus, for the *Sphagnum* mosses desiccation occurs and the time needed before recovery to optimum photosynthetic capacity should be taken into account in our future work. ...

704 likely to reduce the effective LAI of the *Sphagnum* and thus reduce photosynthesis
705 (Walker et al., 2017). Submerged *Sphagnum* can take up carbon derived from CH₄ via
706 symbiotic methanotrophs (Raghoebarsing et al., 2005), but in any cases CO₂ diffusion for
707 photosynthesis will dramatically decrease under water. Larmola et al. (2014) also
708 reported that the activity of oxidizing bacteria provides not only carbon but also nitrogen
709 to peat mosses and, thus, contributes to carbon and nitrogen accumulation in peatlands,
710 which store approximately one-third of the global soil carbon pool. We currently didn't
711 consider this kind of CH₄ associated carbon and nitrogen uptake by *Sphagnum*.

Formatted: Font: Italic

712 The live green *Sphagnum* moss layer buffers the exchange of energy and water at
713 soil surface and regulates the soil temperature and moisture because of its high-water
714 holding capacity and the insulating effect (McFadden et al., 2003; Block et al., 2011;
715 Turesky et al, 2012; Park et al., 2018). Currently, we apply the same method for the
716 hummock and hollow *Sphagnum* water content prediction and can test the model against
717 the measured data when more data are available. Our model still can predict *Sphagnum*

Formatted: Font: Italic

Formatted: Font color: Red

718 water content differences between these microtopographies as expected, with the water
719 content of hollows greater than that of hummocks though. In addition, our model is able
720 to represent the self-cooling effect, although we do not yet have measurements available
721 to validate the model. The relationship of the differences between vegetation temperature
722 (TV) and 2m air temperature (TBOT) (TV-TBOT) and canopy evaporation for both
723 hummock and hollow *Sphagnum* demonstrated that the differences of TV-TBOT was

Formatted: Font: Italic

724 negative and the canopy evaporation had a negative relationship with TV-TBOT (Fig.
725 S3). Moreover, Walker et al., (2017) reported that the function of *Sphagnum* water
726 content to soil water content or to water table depth they used for the SPRUCE site was

Formatted: Font: Italic

727 empirical and may not be representative for peatland ecosystem. To better represent the
728 peatland ecosystem in our model, we will eventually treat the *Sphagnum* mosses as the
729 “top” soil layer with a lower thermal conductivity and higher hydraulic capacity
730 (Beringer et al., 2001; Wu et al., 2016; Porada et al., 2016).

731

732 **5.2 Predicted warming and elevated CO₂ concentration response uncertainties**

733
734 Our model warming simulations suggested that increasing temperature reduced
735 the *Picea* growth but increased the growth of *Larix* under both ambient and elevated
736 atmospheric CO₂ conditions. The main reason for this model difference in response for
737 the two tree species is that despite their similar productivity under ambient conditions,
738 *Picea* has more respiring leaf and fine root biomass because of lower ~~SLA~~, longer leaf
739 longevity, and higher fine root allocation. Therefore, warming results in a much larger
740 increase in maintenance respiration relative to changes in NPP for *Picea* compared to
741 *Larix* (Fig. 5 and Fig. S4). Increased tree growth and productivity in response to the
742 recent climate warming for high-latitude forests has been reported (Myneni et al., 1997,
743 Chen et al. 1999, Wilming et al. 2004, Chavardes, 2013). On the other hand, reductions in
744 tree growth and negative correlations between growth and temperature also have been
745 shown (Barber et al., 2000; Wilmking et al., 2004; Silva et al., 2010; Juday and Alix
746 2012; Girardin et al., 2016; Wolken et al., 2016).

747 Our model also predicted increasing growth of shrubs with increased temperature,
748 similar to simulated increase in shrub cover caused mainly by warmer temperatures and
749 longer growing seasons reported by Miller and Smith (2012) using their model LPJ-
750 GUESS. In addition, several other modelling studies have also found increased biomass

Deleted: specific leaf area

752 production and LAI related to shrub invasion and replacement of low shrubs by taller
753 shrubs and trees in response to increased temperatures in tundra regions (Zhang et al.,
754 2013; Miller and Smith, 2012; Wolf et al., 2008; Porada et al., 2016; Rydssa et al., 2017).

755 The responses of *Sphagnum* mosses to warming simulated by ELM_SPRUCE
756 showed that *Sphagnum* growth in hollows was consistently higher with increased
757 temperatures, where water availability was not limiting. *Sphagnum* growing on
758 hummocks, on the other hand, showed negative warming responses that are related to the
759 strong dependency on water table height. A Recent study of the same SPRUCE site
760 (Norby et al. 2019) had suggested that the hummock-hollow microtopography had a
761 larger influence on *Sphagnum* responses to warming than species-specific traits. In
762 addition, the previous studies had demonstrated that the most dominant mechanism of
763 *Sphagnum* warming response was probably through the effect of warming on depth to the
764 water table and water content of the acrotelm, both of them responded to increasing
765 temperature (Grosvernier et al., 1997; Rydin, 1985; Weltzin et al., 2001; Norby et al.,
766 2019). Moreover, desiccation of capitula due to increased evaporation associated with
767 higher temperatures and vapor pressure deficits can reduce *Sphagnum* growth
768 independent of the water table depth (Gunnarsson et al., 2004). We currently used the
769 same parameters for both hummock and hollow, but could consider species differences in
770 the future. Norby et al. (2019) investigated different *Sphagnum* species at the same site
771 and reported there was no support for the hypothesis that species more adapted to dry
772 conditions (e.g., *S. magellanicum* and *Polytrichum* mainly on hummocks) would be more
773 resistant to the stress and would increase in dominance, and both hummock and hollow

774 *Sphagnum* are declining with warming despite the differences between them. This

Formatted: Font: Italic

Formatted: Font: Italic

Deleted: s

776 declining trend may be in part due to increased shading from the shrub layer, which is
777 expanding with warming (McPartland et al., 2020).
778 Ecosystem warming can have direct and indirect effects on *Sphagnum* moss
779 growth. The growth of *Sphagnum* may be reduced directly by higher air temperature, due
780 to the relatively low temperature optima of moss photosynthesis (Hobbie et al., 1999; Van
781 Gaalen, 2007; Walker et al., 2017). On the other hand, increased shading by the shrub
782 canopy and associated leaf litter could indirectly decrease moss growth (Chapin et al.,
783 1995; Hobbie and Chapin 1998; Van der Wal et al., 2005; Walker et al., 2006; Breeuwer
784 et al., 2008). In contrast, other studies suggest that *Sphagnum* growth can be promoted
785 via a cooling effect of shading on the peat surface, by alleviating photo-inhibition of
786 photosynthesis and also by reducing evaporation stress (Busby et al., 1978; Murray et al.,
787 1993; Man et al., 2008; Walker et al., 2015, Bragazza et al., 2016, Mazziotta et al., 2018).
788 Our model sensitivity analysis also indicated that the parameters of Shrub showing
789 significant sensitivities to *Sphagnum* mosses GPP, indicating that competition between
790 the PFTs for resources might be important. Moreover, ELM_SPRUCE did predict
791 enhancement of shrub and *Larix* tree with increased temperatures with both ambient and
792 elevated CO₂ conditions (~~LAI~~ increasing with warming, Fig. S5). Currently
793 ELM_SPRUCE does not include light competition among multiple PFTs, and thus does
794 not represent cross-PFT shading effects, which may contribute to the warming and
795 elevated CO₂ response differences between our model prediction and observed result of
796 Norby et al. (2019). Meanwhile, we have fixed cover fraction for PFTs in our model may
797 also contribute to the disagreement of predicted and observed warming responses. While

Formatted: Font: Italic

Deleted: the leaf area

Deleted: 3

800 Norby et al. (2019) showed that the fractional cover of different *Sphagnum* species
801 declined with warming.

802 *Sphagnum* mosses are sitting on top of high CO₂ sources. CH₄ can be a significant
803 carbon sources of submerged *Sphagnum* (Raghoebarsing et al., 2005; Larmola et al,
804 2014); refixation of CO₂ derived from decomposition processes also is an important
805 source of carbon for *Sphagnum* (Rydin and Clymo, 1989; Turetsky and Wieder, 1999).
806 The effects of the elevation of atmospheric CO₂ on *Sphagnum* moss are currently
807 disputed, with studies indicating an increase in growth rate (Jauhiainen and Silvde 1999;
808 Heijmans et al. 2001a; Saarnio et al. 2003), decreases in growth rate (Grosvernier et al.
809 2001; Fenner et al. 2007) and no response (Van der Heijden et al. 2000; Hoosbeek et al.
810 2002; Toet et al. 2006). Norby et al. (2019) indicated that no growth stimulation of both
811 hummock and hollow *Sphagnum* under elevated CO₂ condition, but significant negative
812 effects of elevated CO₂ on *Sphagnum* NPP in year 2018 at the same study site.

813 Contrasting responses between *Sphagnum* species are thought to be coupled with the
814 water availability. In contrast, our model results showed that both hummock and hollow
815 *Sphagnum* growths were stimulated by the elevated CO₂ concentration, which may be
816 attributed to the fact that we did not consider the light competition between the PFTS
817 (shrub and tree shading effects) and use a fixed cover fraction of *Sphagnum*.

818 The CO₂ vertical concentration profile is assumed to be uniform in the
819 simulations. In the experiment, the enclosure's regulated additions of pure CO₂ are
820 distributed to a manifold that splits the gas into four equal streams feeding each of the
821 four air handling units (Hanson et al., 2017 Fig. 2a), and is injected into the ductwork of
822 each furnace just ahead of each blower and heat exchanger. Horizontal and vertical

Deleted: v

Formatted: Subscript

Formatted: Subscript

824 mixing within each enclosure homogenizes the air volume distributing the CO₂ along
825 with the heated air. The horizontal blowers in the enclosures together with external wind
826 eddies ensure vertical mixing. We do not have routine automated CO₂ concentration data
827 below 0.5m. The moss layer may well be experiencing higher concentrations than
828 assumed by the model, but such an impact will be minimized during daylight hours.
829 Preliminary isotopic measurements imply a significant fraction of carbon assimilated by
830 the moss may come from subsurface respired CO₂ (i.e., CO₂ with older 14C signatures
831 predating bomb carbon that can only be sourced from deeper peat, Hanson et al., 2017).
832 However, the observed elevated CO₂ response is smaller than simulated (Hanson et al.,
833 2020). Understanding the drivers of elevated CO₂ response or lack thereof is a key topic
834 for future work.
835 To better investigate the *Sphagnum* warming and elevated CO₂ responses, we should
836 also focus on revealing the interactions with shrub and nitrogen availability (Norby et al.,
837 2019). Nitrogen (N₂) fixation is a major source of available N in ecosystems that receive
838 low amounts of atmospheric N deposition, like boreal forests and subarctic tundra (Lindo
839 et al., 2013, Weston et al, 2015, Rousk et al., 2016, Kostka et al., 2016). For example,
840 diazotrophs are estimated to supply 40-60% of N input to peatlands (Vile et at., 2014)
841 with high accumulation of fixed N into plant biomass (Berg et al., 2013). Nevertheless,
842 N₂ fixation is an energy costly process and is inhibited when N availability and reactive
843 nitrogen deposition is high (Gundale et al., 2011; Ackermann et al., 2012; Rousk et al.,
844 2013). This could limit ecosystem N input via the N₂ fixation pathway. We are measuring
845 *Sphagnum* associated N₂ fixation at the SPRUCE site and found that rates decline with
846 increasing temperature (Carrell et al. 2019 Global Change Biology). We are continuing

Formatted: Subscript

Formatted: Subscript

Formatted: Subscript

Formatted: Subscript

Formatted: Subscript

Deleted: Understanding the drivers of elevated CO₂ response or lack thereof is a key topic for future work and we will consider this effect in future assessments of the isotopic carbon budgets for the SPRUCE study

Deleted: S

Formatted: Font: Italic

Formatted: Subscript

852 these measurements to see if they correlate with the GPP empirical relationship from
853 Cleveland *et al.* (1999), or if temperature disrupts that association. Once finished, results
854 will be used to represent N fixation by the *Sphagnum* layer and testing with
855 measurements.

Formatted: Font: Italic

856 It is also encouraging that while we did not use leaf-level gas exchange
857 observations in our optimization, the increased maintenance respiration base rate and
858 temperature sensitivity compared to default (table 2) is largely consistent with pre-
859 treatment leaf level observations (Jensen *et al.*, 2019). In the future, a multi-scale
860 optimization framework that can assimilate leaf and plot-level observations
861 simultaneously should lead to improved model predictions and reduced uncertainties for
862 the treatment simulations. If similar patterns observed in ambient conditions continue
863 during the treatments, incorporating seasonal variations in leaf photosynthetic parameters
864 may also further improve the simulated response to warming (Jensen *et al.*, 2019).

865 Overall, while the sensitivity analysis is useful to indicate the key parameters and
866 mechanisms responsible for uncertainty, our ability to quantify prediction uncertainty is
867 limited because we consider only a single simulation with optimized parameters. Ideally,
868 we should perform a model ensemble that represents the full range of posterior
869 uncertainty over simulations that are consistent with the pre-treatment observations, and
870 also a range of possible future meteorological conditions. This is currently being done for
871 SPRUCE with the TECO carbon cycle model (Jiang *et al.*, 2018), but the computational
872 expense of ELM_SPRUCE currently prohibits this approach. By combining new
873 surrogate modeling approaches (e.g. Lu *et al.*, 2019) with MCMC techniques, it may be
874 possible to achieve this in the near future. This will help to reduce prediction

875 uncertainties, which currently prevail in the future carbon budget of peatlands and its
876 feedback to climate change (McGuire et al., 2009).

877 The algorithms used to represent moss (Williams and Flanagan, 1998) are
878 transferable to and have been applied by other modeling groups in other
879 peatlands. However, we expect that certain parameters will vary, for example, the
880 microtopographic parameters, the relationship between peat moisture and internal water
881 content, and moss properties such as C:N ratio. The parameter sensitivity analysis
882 informs us as to the most important parameters responsible for prediction uncertainty,
883 and can inform how to prioritize these measurements. Collecting these measurements
884 from a variety of sites will be a necessary preliminary exercise. In addition to the
885 simulations aimed at improved understanding of bog response to experimental
886 manipulations at the plot-scale, we are pursuing model implementations at larger spatial
887 scales. The model framework described in this study is capable of performing regional
888 simulations, although the current simulations were designed for mechanistic
889 understanding of *Sphagnum* mosses hydrological and physiological dynamics at the plot-
890 level.

891

892 **6. Summary**

893 In this study, we reported the development of a *Sphagnum* moss PFT and
894 associated processes within the ELM_SPRUCE model. Before being used to examine the
895 ecosystem response to warming and elevated CO₂ at a temperate bog ecosystem, the
896 updated model was evaluated against the observed *Sphagnum* GPP and annual NPP,
897 aboveground tree biomass and shrub stem biomass. The new model can capture the

Deleted: e.g.

899 seasonal dynamics of moss *Sphagnum* GPP, but with lower peak GPP compared to site-
900 level observations, and can predict reasonable annual values for *Sphagnum* NPP but with
901 lower interannual variation. Our model largely agrees with observed tree and shrub
902 biomass. The model predicts that different PFTs responded differently to warming levels
903 under both ambient and elevated CO₂ concentration conditions. The NPP of the two
904 dominant tree PFTs (black spruce and *Larix*) showed contrasting responses to warming
905 scenarios (increasing with warming for *Larix* but decreasing for black spruce), while
906 shrub NPP had similar warming response to *Larix*. Hummock and hollow *Sphagnum*
907 showed opposite warming responses: hollow *Sphagnum* shows generally higher growth
908 with warming, but the hummock *Sphagnum* demonstrates more variability and strong
909 dependence with water table height. The ELM predictions further suggest that the effects
910 of CO₂ fertilization can change the direction of the warming response for the bog
911 peatland ecosystem, though observations of *Sphagnum* species at the site does not yet
912 appear to support this (Norby et al. 2019).

913 Data availability. The model code we used is available here:
914 https://github.com/dmricciuto/CLM_SPRUCE. The datasets and scripts were used for the figures
915 is here: https://github.com/dmricciuto/CLM_SPRUCE/tree/master/analysis/Shietal2020
916
917

918 **Acknowledgements**

919 Research was supported by the U. S. Department of Energy, Office of Science,
920 Biological and Environmental Research Program. Oak Ridge National Laboratory is
921 managed by UT-Battelle, LLC, for the US Department of Energy under contract DE-
922 AC05-00OR22725.

923

924 **References:**

- 925 Ackermann, K., Zackrisson, O., Rousk, J., Jones, D. L., and DeLuca, T. H.: N₂ fixation
926 in feather mosses is a sensitive indicator of N deposition in boreal forests, *Ecosystems*,
927 15, 986-998, 2012.
- 928 Barber, V. A., Juday, G. P., and Finney, B. P.: Reduced growth of Alaskan white spruce
929 in the twentieth century from temperature-induced drought stress, *Nature*, 405,668-
930 673, 2000.
- 931 Beringer, J., Lynch, A., Chapin, F., Mack, M., and Bonan, G.: The Representation of
932 Arctic Soils in the Land Surface Model: The Importance of Mosses, *J. Climate*, 14,
933 3324-3335, doi:10.1175/1520-0442(2001)014<3324:TROASI>2.0.CO;2, 2001.
- 934 Berg, A., Danielsson, A., and Sevansson, B.H.: Transfer of fixed-N from N₂-fixing
935 cyanobacteria associated with moss sphagnum riparium results in enhanced growth of
936 the moss, plant and soil, 362, 271-278, <https://doi.org/10.1007/s11104-012-1278-4>,
937 2013.
- 938 Blok, D., Heijmans, M., Schaepman-Strub, G., Van Ruijven, J., Parmentier, F.,
939 Maximov, T., and Berendse, F.: The cooling capacity of mosses: Controls on water
940 and energy fluxes in a Siberian tundra site, *Ecosystems*, 14, 1055-1065, 2011.
- 941 Bond-Lamberty, B., Peckham, S. D., Ahl, D. E., and Gower, S. T.: Fire as the dominant
942 driver of central Canadian boreal forest carbon balance, *Nature*, 450, 89-92, 2007.
- 943 Bragazza, L., Buttler, A., Robroek, B. J., Albrecht, R., Zaccone, C., Jassey, V. E., and
944 Signarbieux, C.: Persistent high temperature and low precipitation reduce peat carbon
945 accumulation, *Global Change Biology*, 22, 4114-4123,
946 <https://doi.org/10.1111/gcb.13319>, 2016.
- 947 Breeuwer, A., Heijmans, M. M., Robroek, B. J., and Berendse, F.: The effect of
948 temperature on growth and competition between *Sphagnum*
949 species, *Oecologia*, 156(1), 155-167, doi:10.1007/s00442-008-0963-8, 2008.
- 950 Brown, S. M., Petrone, R. M., Mendoza, C., and Devito, K. J.: Surface vegetation
951 controls on evapotranspiration from a sub-humid Western Boreal Plain wetland,
952 *Hydrological Processes*, 24(8), 1072-1085, 2010.
- 953 Busby, J.R., Bliss, L.C., and Hamilton, C.D.: Microclimate control of growth rates and
954 habitats of the Boreal Forest Mosses, *Tomenthypnum nitens* and *Hylocomium*
955 *splenden*, *Ecol Monogr*, 48, 95-110, 1978.
- 956 Burrows, S.M., Maltrud, M.E., Yang, X., Zhu, Q., Jeffery, N., Shi, X., Ricciuto, D.M.,
957 Wang, S., Bisht, G., Tang, J., Wolfe, J. D., Harrop, B. E., Singh, B., Brent, L., Zhou,
958 Tian, Cameron-Smith P. J., Keen, N., Collier, N., Xu, M., Hunke, E.C., Elliott, S.M.,
959 Turner, A.K., Li, H., Wang, H., Golaz, J.-C., Bond-Lamberty, B., Hoffman, F.M.,
960 Riley, W.J., Thornton, P.E., Calvin, K., and Leung, L.R.: The DOE E3SM coupled

Formatted: Indent: Left: 0", Hanging: 0.19"

961 model v1.1 biogeochemistry configuration: overview and evaluation of coupled
 962 carbon-climate experiments, *J. Adv. Model Earth Sy.*, 12, e2019MS001766,
 963 <https://doi.org/10.1029/2019MS001766>, 2020.

964 Gorham, E.: Northern peatlands: role in the carbon cycle and probable responses to
 965 climatic warming, *Ecological Applications*, 1, 182-195, 1991.

966 Camill, P. and Clark, J. S.: Long-term perspectives on lagged ecosystem responses to
 967 climate change: permafrost in boreal peatlands and the grassland/woodland boundary,
 968 *Ecosystems*, 3, 534–544, 2000.

969 Chadburn, S., Burke, E., Essery, R., Boike, J., Langer, M., Heikenfeld, M., Cox, P., and
 970 Friedlingstein, P.: An improved representation of physical permafrost dynamics in
 971 the JULES land-surface model, *Geosci. Model Dev.*, 8, 1493–1508, doi:10.5194/gmd-
 972 8-1493-2015, 2015.

973 Chapin, F. S. III, Shaver, G.R., Giblin, A.E., Nadelhoffer, K.J., and Laundre, J.A.:
 974 Responses of Arctic tundra to experimental and observed changes in climate, *Ecology*,
 975 76, 694-711, 1995.

976 Carrell, A.A., Kolton, M., Warren, M.J., Kostka, J.E., and Weston, D. J.: Experimental
 977 warming alters the community composition, diversity, and N₂ fixation activity of peat
 978 moss (*Sphagnum fallax*) microbiomes, *Glob. Change Biol.*, 25, 2993-3004,
 979 doi:10.1111/gcb.14715, 2019.

980 Chavardes, R. D., Daniels, L. D., Waeber, P. O., Innes, J. L., and Nitschke, C. R.:
 981 Unstable climate-growth relations for white spruce in southwest Yukon, Canada,
 982 *Climatic Change*, 116, 593-611, 2013.

983 Chen, W. J., Black, T. A., Yang, P.C. Barr, A.G. Neumann, H. H., Nešić, Z., Blanken, P.
 984 D. Novak, M. D., Eley, J., Ketler, R., and Cuenca, R. H.: Effects of climatic variability
 985 on the annual carbon sequestration by a boreal aspen forest, *Glob. Change Biol.*, 5, 41-
 986 53, 1999.

987 [Cleveland, C. C., Townsend, A. R., Schimel, D. S., Fisher, H., Howarth, Lars O., H.,](#)
 988 [Perakis, S. S., Latty, E. F., Von Fishcher, J. C., Elseroad, A., and Wasson, M. F.:](#)
 989 [Global patterns of terrestrial biological nitrogen \(N₂\) fixation in natural ecosystem,](#)
 990 [Global Biogeochemical Cycles, 13\(2\), 623-645, 1999.](#)

991 Clymo, R. S. and Hayward, P.M.: The ecology of Sphagnum, in: *Bryophyte Ecology*,
 992 edited by: Smith, A. I. E., Chapman and Hall Ltd., London, New York, 229-289, 1982.

993 Collatz, G.J., Ball, J.T., Grivet, C. and Berry, J.A.: Physiological and environmental-
 994 regulation of stomatal conductance, photosynthesis and transpiration - a model that
 995 includes a laminar boundary-layer, *Agricultural and Forest Meteorology*, 54, 107-
 996 136, 1991.

997 Collatz, G.J., Ribas-Carbo, M. and Berry, J.A.: Coupled photosynthesis- stomatal model
 998 for leaves of C4 plants, *Australian Journal of Plant Physiology*, 19, 519-538, 1992.

- Moved down [1]: P. O.
- Deleted: L. D.
- Deleted: J. L.
- Moved down [2]: C. R.
- Moved (insertion) [1]
- Moved (insertion) [2]
- Deleted:
- Deleted: .
- Formatted: Subscript

1005 Cornelissen, H.C., Lang, S.I., Soudzilovskaia, N.A., and During, H.J.: Comparative
1006 cryptogam ecology: a review of bryophyte and lichen traits that drive
1007 biogeochemistry, *Annals of Botany*, 99, 987–1001, 2007.

1008 Davidson, E. A. and Janssens, I. A.: Temperature sensitivity of soil carbon decomposition
1009 and feedbacks to climate change, *Nature*, 440, 165-173, 2006.

1010 Dorrepaal, E., Toet, S., van Logtestijn, R. S. P., Swart, E., van de Weg, M. J., Callaghan,
1011 T. V., and Aerts, R.: Carbon respiration from subsurface peat accelerated by climate
1012 warming in the sub- arctic, *Nature*, 460, 616-619, 2009.

1013 Druel, A., Peylin, P., Krinner, G., Ciais, P., Viovy, N., Peregon, A., Barstrikov, V.,
1014 Kosykh, N., Mironycheva-Tokareva, N.: Towards a more detailed representation of
1015 high-latitude vegetation in the global land surface model ORCHIDEE (ORC-HL-
1016 VEGv1.0), *Geoscientific Model Development*, 10(12), 4693–4722,
1017 <https://doi.org/10.5194/gmd-10-4693-2017>, 2017.

1018 Duarte, H. F., Raczka, B. M., Ricciuto, D. M., Lin, J. C., Koven, C. D., Thornton, P. E.,
1019 Bowling, D. R., Lai, C. T., Bible, K. J. and Ehleringer, J. R.: Evaluating the
1020 Community Land Model (CLM4.5) at a coniferous forest site in northwestern United
1021 States using flux and carbon-isotope measurements, *Biogeosciences*, 14(18): 4315-
1022 4340, DOI: 10.5194/bg-14-4315-2017, 2017.

1023 Euskirchen, E.S., McGuire, A.D., Chapin, F.S. III, Yi, S., and Thompson, C.C.: Changes
1024 in vegetation in northern Alaska under scenarios of climate change, 2003–2100:
1025 implications for climate feedbacks, *Ecological Applications* 19: 1022-1043, 2009.

1026 Farquhar, G.D., von Caemmerer, S. and Berry, J.A.: A biochemical model of
1027 photosynthetic CO₂ assimilation in leaves of C₃ species. *Planta*, 149, 78-90, 1980.

1028 Fenner, N., Ostle, N.J., McNamara, N., Sparks, T., Harmens, H., Reynolds, B., and
1029 Freeman, C.: Elevated CO₂ effects on peat- land plant community carbon dynamics
1030 and DOC production, *Ecosystem*, 10,635-647,2007.

1031 Frolking, S. and Roulet, N.T.: Holocene radiative forcing impact of northern peatland
1032 carbon accumulation and methane emissions, *Glob. Change Biol.* 13, 1079-1088,
1033 2007.

1034
1035 Girardin, M. P., Bouriaud, O., Hogg, E. H., Kurz, W., Zimmermann, N. E., Metsaranta, J.
1036 M., Jong, Rogier de, Frank, D. C., Esper, J., Büntgen, U., Guo, X., and Bhatti, J.: No
1037 growth stimulation of Canada’s boreal forest under half-century of combined warming
1038 and CO₂ fertilization, *Proceedings of the National Academy of Science*, 113(52),
1039 E8406–E8414, 2016.

1040 Goetz, J.D., and Price, J.S.: Role of morphological structure and layering of Sphagnum
1041 and Tomenthypnum mosses on moss productivity and evaporation rates, *Canadian
1042 Journal of Soil Sciences*. DOI:10.4141/ CJSS-2014-092, 2015.

Deleted: Dimitrov, D. D., Grant, R. F., LaFleur, P. M., and Humphreys, E.: Modelling the effects of hydrology on gross primary productivity and net ecosystem productivity at Mer Bleue bog, *J. Geophys. Res.-Biogeo*, 116, G04010, doi:10.1029/2010JG001586, 2011. ¶

Deleted: Frolking, S., Talbot, J., Jones, M. C., Treat, C. C., Kauffman, Tuittila E.-S., and Roulet, N.: Peatlands in the Earth’s 21st century coupled climate-carbon system, *Environ. Rev.*, 19, 371-396, 2011. ¶

- 1052 Golaz, J.-C., Caldwell, P. M., Van Roekel, L. P., Petersen, M. R., Tang, Q., Wolfe, J. D.,
1053 Abeshu, G., Anantharaj, V., Asay-Davis, X. S., Bader, D.C., Baldwin, S. A., Bisht, G.,
1054 Bogenschutz, P. A., Branstetter, M., Brunke, M., A., Brus, S.R., Burrows, S.M.,
1055 Cameron-Smith P. J., Donahue, A. S., Deakin, M., Easter, R. C., Evans, K. J., Feng,
1056 Y., Flanner, M., Foucar, J., G., Fyke, J. G., Griffin, B. M., Hannay, C., Harrop, B. E.,
1057 Hoffman, M. J., Hunke, E. C., Jacob, R. L., Jacobsen, D. W., Jeffery, N., Jones, P. W.,
1058 Klein, S. A., Larson, V. E., Leung, L. R., Li, H., Lin, W., Lipscomb, W.H., Ma, P.-L.,
1059 Mahajan, S., Maltrud, M., E., Mametjanov, A., McClean, J. L., McCoy, R. B., Neale,
1060 R.B., Price, S. F., Qian, Y., Rasch, P. J., Reeves Eyre, J.E.J., Riley, W. J., Ringler, T.
1061 D., Roberts, A. F., Roesler, E. L., Salinger, A. G., Shaheen, Z., Shi, X., Singh, B.,
1062 Tang, J., Taylor, M. A., Thornton, P. E., Tuner, A. K., Veneziani, M., Wan, H., Wang,
1063 H., Wang, S., Williams, D. N., Wolfram, P. J., Worley, P. H., Xie, S., Yang, Y., Yoon,
1064 J.-H., Zelinka, M. D., Zender, C. S., Zeng, X., Zhang, C., Zhang, K., Zhang, Y.,
1065 Zheng, X., Zhou, T., Zhu, Q.: The DOE E3SM coupled model version 1: Overview
1066 and evaluation at standard resolution, *J. Adv. Model Earth Sy*, 11(7), 2089-2129,
1067 <https://doi.org/10.1029/2018MS001603>, 2019.
- 1068 Gong, J., Roulet, N., Frolking, S., Peltola, H., Laine, A.M., Kokkonen, N., and Tuittila,
1069 E.-S.: Modelling the habitat preference of two key sphagnum species in a poor fen as
1070 controlled by capitulum water retention, *Biogeosciences Discussions*,
1071 <https://dio.org/10.5194/bg-2019-366>, 2019.
- 1072 Gorham, E.: Northern peatlands: role in the carbon cycle and probable responses to
1073 climatic warming, *Ecological Applications*, 1, 182-195, 1991.
- 1074 Grant, R. F., Desai, A. R., and Sulman, B. N.: Modelling contrasting responses of
1075 wetland productivity to changes in water table depth, *Biogeosciences*, 9, 4215-4231,
1076 2012.
- 1077 Granath, G., Limpens, J., Posch, M., Mücher, S., and De Vries, W.: Spatio-temporal
1078 trends of nitrogen deposition and climate effects on Sphagnum productivity in
1079 European peatlands, *Environmental Pollution*, 187, 73-80, [https://doi.org/10.1016/j.](https://doi.org/10.1016/j.envpol.2013.12.023)
1080 [envpol.2013.12.023](https://doi.org/10.1016/j.envpol.2013.12.023), 2014
- 1081 Griffiths, N. A., and Sebestyen, S. D.: Dynamic vertical
1082 profiles of peat porewater chemistry in a northern peatland, *Wetlands*, 36(6), 1119-
1130, 2016.
- 1083 Griffiths, N. A., and Sebestyen, S. D.: Dynamic vertical profiles of peat porewater
1084 chemistry in a northern peatland, *Wetland*, 36, 1119-1130, doi:10.1007/s13157-016-
1085 0829-5, 2016.
- 1086 Griffiths, N. A., Hanson, P. J., Ricciuto, Iversen, C. M., Jensen, A.M., Malhotra, A.,
1087 McFarlane, K. J., Norby, R. J., Sargsyan, K., Sebestyen, S. D., Shi, X., Walker, A. P.,
1088 Ward, E. J., Warren, J. M., and Weston, D. J.: Temporal and spatial variation in
1089 peatland carbon cycling and implications for interpreting responses of an ecosystem-
1090 scale warming experiment, *Soil Sci. Soc. Am. J.*, 81(6), 1668-1688,
1091 doi:10.2136/sssaj2016.12.0422, 2018.
- 1092 Grosvernier, P., Matthey, Y., and Buttler, A.: Growth potential of three Sphagnum
1093 species in relation to water table level and peat properties with implications for their
1094 restoration in cut-over bogs, *Journal of Applied Ecology*, 34(2), 471-483.
1095 <https://doi.org/10.2307/2404891>, 1997.

Formatted: Indent: Left: 0", Hanging: 0.19"

1096 Grosvernier, P.R., Mitchell, E.A.D., Buttler, A., Gobat, J.M.: Effects of elevated CO₂ and
1097 nitrogen deposition on natural regeneration processes of cut-over ombrotrophic peat
1098 bogs in the Swiss Jura mountains, *Glob Change Prot Areas* 9, 347 – 35, 2001.

1099 Gundale, M.J., DeLuca, T.H., and Nordin, A.: Bryophytes attenuate anthropogenic
1100 nitrogen inputs in boreal forests, *Glob. Change Biol.*, 17, 2743-2753, 2011.

1101 Gunnarsson, U., Granberg, G., & Nilsson, M.: Growth, production and interspecific
1102 competition in *Sphagnum*: effects of temperature, nitrogen and sulphur treatments on a
1103 boreal mire, *New Phytologist*, 163(2), 349-359, [https://doi.org/10.1111/j.1469-](https://doi.org/10.1111/j.1469-8137.2004.01108.x)
1104 [8137.2004.01108.x](https://doi.org/10.1111/j.1469-8137.2004.01108.x), 2004.

1105 Hanson, P. J., Riggs, J.S., Nettles, W. R., Krassovski, M. B., and Hook L. A.: SPRUCE
1106 deep peat heating (DPH) environmental data, February 2014 through July 2015, Oak
1107 Ridge National Laboratory, TES SFA, U.S. Department of Energy, Oak Ridge,
1108 Tennessee, U.S.A. <https://doi.org/10.3334/CDIAC/spruce.013>, 2015a.

1109 Hanson, P.J., Riggs, J.S. Dorrance, C., Nettles, W.R., and Hook, L.A.: SPRUCE
1110 Environmental Monitoring Data: 2010-2016. Carbon Dioxide Information Analysis
1111 Center, Oak Ridge National Laboratory, U.S. Department of Energy, Oak Ridge,
1112 Tennessee, U.S.A. <http://dx.doi.org/10.3334/CDIAC/spruce.001>, 2015b.

1113 Hanson, P. J., Riggs, J.S., Nettles, W.R., Phillips, J.R., Krassovski, M.B., Hook, L.A.,
1114 Gu, L., Richardson, A.D., Aubrecht, D.M., Ricciuto, D.M., Warren, J.M., and Barbier,
1115 C.: Attaining whole-ecosystem warming using air and deep-soil heating methods with
1116 an elevated CO₂ atmosphere, *Biogeosciences*, 14, 861-883, 2017.

1117

1118 Hanson, P.J., Phillips, J.R., Wullschelger, S. D., Nettles, W. R., Warren, J. M., Ward, E.
1119 J.: SPRUCE Tree Growth Assessments of Picea and Larix in S1-Bog Plots and
1120 SPRUCE Experimental Plots beginning in 2011, Oak Ridge National Laboratory, TES
1121 SFA, U.S. Department of Energy, Oak Ridge, Tennessee,
1122 U.S.A. <https://doi.org/10.25581/spruce.051/1433836>, 2018a.

1123

1124 Hanson, P.J., Phillips, J.R., Brice, D.J., and Hook, L.A.: SPRUCE Shrub-Layer Growth
1125 Assessments in S1-Bog Plots and SPRUCE Experimental Plots beginning in
1126 2010. Oak Ridge National Laboratory, TES SFA, U.S. Department of Energy, Oak
1127 Ridge, Tennessee, U.S.A. <https://doi.org/10.25581/spruce.052/1433837>, 2018b.

1128 Hanson, P. J., Griffiths, N.A., Iversen, C.M., Norby, R. J., Sebestyen, S. D., Phillips,
1129 Jeffrey, J. R., Chanton, P., Kolka, R. K., Malhotra, A., Oleheiser, K. C., Warren, J. M.,
1130 Shi, X., Yang, X., Mao, J., and Ricciuto, D., M.: Rapid net carbon loss from a whole-
1131 ecosystem warmed peatland. *AGU Advances*, 1, e2020AV000163,
1132 <https://doi.org/10.1029/2020AV000163>, 2020.

1133 Heijmans, M., Arp, W.J., Berendse, F.: Effects of elevated CO₂ and vascular plants on
1134 evapotranspiration in bog vegetation, *Glob Change Biol* 7:817 – 827, 2001.

Formatted: Indent: Left: 0", Hanging: 0.19"

Deleted: Hanson, P. J., Gill, A. L., Xu, X., Phillips, J. R., Weston, D. J., Kolka, R. K., Riggs, J. S., and Hook, L. A.: Intermediate-scale community-level flux of CO₂ and CH₄ in a Minnesota peatland: putting the SPRUCE project in a global context, *Biogeochemistry*, 129(3), 255-272, 2016.

- 1140 Heijmans, M.M.P.D., Arp, W.J., and Chapin, F.S. III.: Carbon dioxide and water vapour
 1141 exchange from understory species in boreal forest, *Agricultural and Forest*
 1142 *Meteorology* 123,135-147, DOI:10.1016/j. agrformet.2003.12.006, 2004a.
- 1143 Heijmans, M.M.P.D, Arp, W.J., and Chapin, F.S. III.: Controls on moss evaporation in a
 1144 boreal black spruce forest. *Global Biogeochemical Cycles* 18(2), 1-8,
 1145 DOI:10.1029/2003GB002128, 2004b.
- 1146 Heijmans, M.M. P. D., Mauquoy, D., van Geel, B., and Berendse, F.: Long-term effects
 1147 of climate change on vegetation and carbon dynamics in peat bogs. *Journal of*
 1148 *Vegetation Science* 19, 307-320, 2008.
- 1149 Hobbie, S.E., and Chapin, F.S. III.: The response of tundra plant biomass, aboveground
 1150 production, nitrogen, and CO₂ flux to experimental warming, *Ecology*, 79,1526-1544,
 1151 1998.
- 1152 Hobbie, S.E., Shevtsova, A., and Chapin, F.S.III.: Plant responses to species removal and
 1153 experimental warming in Alaskan Tus- sock Tundra. *Oikos* 84,417-434, 1999.
- 1154 Hoosbeek, M.R., Van Breemen, N., Vasander, H., Buttler, A., Berendse, F.: Potassium
 1155 limits potential growth of bog vegetation under elevated atmospheric CO₂ and N
 1156 deposition, *Glob. Change Biol.*, 8,1130-1138, [https://doi.org/10.1046/j.1365-](https://doi.org/10.1046/j.1365-2486.2002.00535.x)
 1157 [2486.2002.00535.x](https://doi.org/10.1046/j.1365-2486.2002.00535.x), 2002.
- 1158 Ise, T., Dunn, A. L., Wofsy, S. C., and Moorcroft, P. R.: High sensitivity of peat
 1159 decomposition to climate change through water table feedback, *Nat. Geosci.*, 1, 763-
 1160 766, 2008.
- 1161 Jauhiainen, J., Silvola, J.: Photosynthesis of *Sphagnum fuscum* at long-term raised CO₂
 1162 concentrations, *Annales Botanici Fennici*, 36,11-19, 1999.
- 1163 Jensen, A.M., Warren, J. M., Hook, L. A., Wulschleger, S. D., Brice, D.J., Childs, J.,
 1164 and Vander Stel, H.M.: SPRUCE S1 Bog Pretreatment Seasonal Photosynthesis and
 1165 Respiration of Trees, Shrubs, and Herbaceous Plants, 2010-2015, Oak Ridge National
 1166 Laboratory, TES SFA, U.S. Department of Energy, Oak Ridge, Tennessee, U.S.A.,
 1167 <https://doi.org/10.3334/CDIAC/spruce.008>, 2018.
- 1168 Jensen, A.M., Warren, J. M., King, A., Ricciuto, D.M., Hanson, P. J., and Wulschleger,
 1169 S. D.: Simulated projections of boreal forest peatland ecosystem productivity are
 1170 sensitive to observed seasonality in leaf phenology, *Tree Physiology*, 39(4), 556-572,
 1171 doi: 10.1093/treephys/tpy140, 2019.
- 1172 Jiang, J., Huang, Y., Ma, S., Stacy, M., Shi, Z., Ricciuto, D. M., Hanson, P. J., and Luo,
 1173 Y.: Forecasting Responses of a Northern Peatland Carbon Cycle to Elevated CO₂ and
 1174 a Gradient of Experimental Warming, *J. Geophys. Res.-Biogeo*, 123(3), 1057-1071,
 1175 doi: 10.1002/2017JG004040, 2018.

Formatted: Indent: Left: 0", Hanging: 0.19"

Formatted: Indent: Left: 0", Hanging: 0.19"

- 1176 Juday, G. P., and Alix, C.: Consistent negative temperature sensitivity and positive
 1177 influence of precipitation on growth of floodplain *Picea glauca* in Interior Alaska,
 1178 *Canadian Journal of Forest Research*, 42, 561-573, 2012.
 1179
- 1180 Kostka, J.E., Weston, D.J., Glass, J.B., Lilleskov, E.A., Shaw, A.J., and Turetsky, M.R.:
 1181 The Sphagnum microbiome: new insights from an ancient plant lineage, *New*
 1182 *Phytologist*, 211(1):57-64, 2016
- 1183 Kuiper, J. J., Mooij, W. M., Bragazza, L., and Robroek, B. J.: Plant functional types
 1184 define magnitude of drought response in peatland CO₂ exchange, *Ecology*, 95, 123-
 1185 131, <https://doi.org/10.1890/13-0270.1>, 2014.
- 1186 Lafleur, P. M., Hember, R. A., Admiral, S. W., and Roulet, N. T.: Annual and seasonal
 1187 variability in evapotranspiration and water table at a shrub-covered bog in southern
 1188 Ontario, Canada, *Hydrol. Process.*, 19, 3533–3550, <https://doi.org/10.1002/hyp.5842>,
 1189 2005.
- 1190 Larmola, T., Leppänen, S. M., Tuittila, E.-Stiina, Aarva, M., Merilä, P., Fritze, H.,
 1191 Tiirola, M.: Methanotrophy induces nitrogen fixation during peatland development,
 1192 *PNAS*, 734-739, www.pnas.org/cgi/dio/10.1073/pnas.1314284111, 2014.
- 1193 Launiainen, S., Katul, G. G., Lauren, A., and Kolari, P.: Coupling boreal forest CO₂, H₂O
 1194 and energy flow by a vertically structured forest canopy-Soil model with separate
 1195 bryophyte layer. *Ecological Modelling*, 312, 385-405.
 1196 <https://doi.org/10.1016/j.ecolmodel.2015.06.007>, 2015.
- 1197 Lindo, Z., and Gonzalez, A.: The bryosphere: an integral and influential component of the
 1198 earth's biosphere, *Ecosystems*, 13, 612–627, 2010.
- 1199 Lindo, Z., Nilsson, M.C., and Gundale, M.J.: Bryophyte-cyanobacteria associations as
 1200 regulators of the northern latitude carbon balance in response to global change, *Glob.*
 1201 *Change Biol.*, 19(7),2022-35, 2013.
- 1202 Lu, D., Ricciuto, D.M., Stoyanov, M., and Gu, L.: Calibration of the E3SM Land Model
 1203 Using Surrogate-Based Global Optimization, *J Adv Model Earth Sy*, 10(6), 1337-
 1204 1356, doi: 10.1002/2017ms001134, 2018.
- 1205 Lu, D., and Ricciuto, D.M.: Efficient surrogate modeling methods for large-scale Earth
 1206 system models based on machine-learning techniques, *Geosci Model Dev*, 12(5),
 1207 1791-1807, doi: 10.5194/gmd-12-1791-2019, 2019.
- 1208 Man, R., Kayahara, G.J., Rice, J.A., and MacDonald, G.B.: Eleven- year responses of a
 1209 boreal mixedwood stand to partial har- vesting: light, vegetation, and regeneration
 1210 dynamics, *For Ecol Manag* 255,697-706, 2008.

Deleted: Limpens, J., Berendse, F., Blodau, C., Canadell, J. G., Freeman, C., Holden, J., Roulet, N., Rydin, H., and Schaepman-Strub, G.: Peatlands and the carbon cycle: From local processes to global implications-A synthesis, *Biogeosciences*, 5(5), 1475-1491, doi:10.5194/bg-5-1475-2008, 2008.

- 1217 Mazziotto, A., Granath, G., Rydin, H. and Bengtsson F.: Scaling functional traits to
1218 ecosystem processes: Towards a mechanistic understanding in peat mosses, *Journal of*
1219 *Ecology*, DOI:10.1111/1365-2745.13110, 2018.
- 1220 Metcalfe, D. B., Ricciuto D. M., Palmroth, S., Campbell, Hurry, C., V., Mao, J., Keel, S.
1221 G., Linder, S., Shi, X., Näsholm, T., Ohlsson, K. E. A., Blackburn, M., Thornton, P. E.
1222 and Oren, R.: Informing climate models with rapid chamber measurements of forest
1223 carbon uptake, *Global Change Biology*, 23(5), 2130-2139, DOI: 10.1111/gcb.13451,
1224 2017.
- 1225 McFadden, J.P., Eugster, W., Chapin, F.S.III.: A regional study of the controls on water
1226 vapor and CO₂ exchange in Arctic tundra, *Ecology*, 84,2762-76, 2003.
- 1227 McGuire, A. D., Anderson, L. G., Christensen, T. R., Dallimore, S., Guo, L., Hayes, D.
1228 J., Heimann, M., Lorenson, T. D., Macdonald, R. W. and Roulet, N.: Sensitivity of the
1229 carbon cycle in the Arctic to climate change, *Ecol. Monogr.*, 79, 523-555, 2009.
- 1230 [McPartland, M. Y., Montgomery, R. A., Hanson, P. J., Phillips, J. R., Kolka, R., Palik B.:](#)
1231 [Vascular plant species response to warming and elevated carbon dioxide in a boreal](#)
1232 [peatland. *Environ. Res. Lett.*, <https://doi.org/10.1088/1748-9236/abc4fb>, 2020.](#)
- 1233 Miller, P. A. and Smith, B.: Modelling Tundra Vegetation Response to Recent Arctic
1234 Warming, *Ambio*, 41, 281-291, <https://doi.org/10.1007/s13280-012-0306-1>, 2012.
- 1235 Mokhov, I.I., Eliseev, A.V., and Denisov, S.N.: Model diagnostics of variations in
1236 methane emissions by wetlands in the second half of the 20th century based on
1237 reanalysis data, *Dokl. Earth Sci.*, 417(1),1293-1297, 2007.
- 1238 Moore, T.R., Roulet, N.T., and Waddington, J.M.: Uncertainty in predicting the effect of
1239 climate change on the carbon cycling of Canadian peatlands, *Clim. Change*, 40, 229-
1240 245, 1998.
- 1241 Myneni, R. B., Keeling, C. D., Tucker, C. J., Asrar, G., and Nemani, R. R.: Increased
1242 plant growth in the northern high latitudes from 1981 to 1999, *Nature*, 386,698-702,
1243 1997.
- 1244 Murray, K.J., Tenhunen, J.D., and Nowak, R.S.: Photoinhibition as a control on
1245 photosynthesis and production of Sphagnum mosses, *Oecologia*, 96,200-207, 1993.
- 1246 Nichols, J.E., and Peteet, D.M.: Rapid expansion of northern peatlands and doubled
1247 estimate of carbon storage, *Nat. Geosci.* 12, 917-921, doi:10.1038/s41561-019-0454-z,
1248 2019.
- 1249 Nilsson, M.C., and Wardle, D.A.: Understorey vegetation as a forest ecosystem driver:
1250 evidence from the northern Swedish boreal forest, *Frontiers in Ecology and the*
1251 *Environment*, 3, 421-428, 2005.
- 1252 Norby, R.J., and Childs, J.: Sphagnum productivity and community composition
1253 in the SPRUCE experimental plots. *Carbon Dioxide Information Analysis*

Formatted: Subscript

- 1254 Center, Oak Ridge National Laboratory, U.S. Department of Energy, Oak
1255 Ridge, Tennessee, U.S.A. <http://dx.doi.org/10.3334/CDIAC/spruce.xxx>, 2017.
- 1256 Norby, R.J., Childs, J., Hanson, P.J., and Warren, J.M.: Rapid loss of an ecosystem
1257 engineer: Sphagnum decline in an experimentally warmed bog, *Ecology and*
1258 *Evolution*, 9(22), 12571-12585, <https://doi.org/10.1002/ece3.5722>, 2019.
- 1259 Nungesser, M. K.: Modelling microtopography in boreal peatlands: Hummocks and
1260 hollows, *Ecol. Model.*, 165(2-3), 175-207, 2003.
- 1261
- 1262 Oechel, W.C., and Van Cleve, K.: The role of bryophytes in nutrient cycling in the taiga,
1263 in *Ecological Studies*, Vol. 57: Forest Ecosystems in the Alaskan Taiga, edited by:
1264 Van Cleve, K., Chapin III, F. S., Flanagan, P.W., Viereck, L.A., and Dyrness, C.T.,
1265 Springer-Verlag, New York, 121-137, 1986.
- 1266 Oleson, K. W., Lawrence, D. W., Bonan, G. B., Drewniak, B., Huang, M., Koven, C. D.,
1267 Levis, S., Li, F., Riley, W. J., Subin, Z. M., Swenson, S. C., Thornton, P. E., Bozbiyik,
1268 A., Fisher, R., Heald, C. L., Kluzek, E., Lamarque, J., Lawrence, P. J., Leung, L. R.,
1269 Lipscomb, W., Muszala, S., Ricciuto, D. M., Sacks, W., Sun, Y., Tang, J., and Yang,
1270 Z.: Technical description of version 4.5 of the Community Land Model (CLM),
1271 NCAR/TN-503+STR, NCAR Technical Note, 2013.
- 1272 Park, H., Launiainen, S., Konstantinov, P. Y., Iijima, Y., and Fedorov, A. N.: Modeling
1273 the effect of moss cover on soil temperature and carbon fluxes at a tundra site in
1274 northeastern Siberia, *J. Geophys. Res.-Bioge*, 123, 3028-3044, <https://doi.org/10.1029/2018JG004491>, 2018.
- 1275
- 1276 Parsekian, A. D., Slater, L., Ntarlagiannis, D., Nolan, J., S. Sebestyen, D., Kolka, R. K.,
1277 and Hanson, P. J.: Uncertainty in peat volume and soil carbon estimated using ground-
1278 penetrating radar and probing. *Soil Sci. Soc. Am. J.*, 76, 1911-1918. DOI:
1279 10.2136/sssaj2012.0040, 2012.
- 1280 Pastor, J., Peckham, B., Bridgham, S., Weltzin, J., and Chen, J.: Plant community
1281 dynamics, nutrient cycling, and alternative stable equilibria in peatlands, *The*
1282 *American Naturalist* 160, 553-568, 2002.
- 1283 Petrone, R., Solondz, D., Macrae, M., Gignac, D., and Devito, K.J.: Microtopographical
1284 and canopy cover controls on moss carbon dioxide exchange in a western boreal plain
1285 peatland, *Ecohydrology*, 4, 115-129, 2011.
- 1286 Porada, P., Weber, B., Elbert, W., Pöschl, U., and Kleidon, A.: Estimating global carbon
1287 uptake by lichens and bryophytes with a process-based model, *Biogeosciences*, 10,
1288 6989–7033, doi:10.5194/bg-10-6989-2013, 2013.
- 1289 Porada, P., Ekici, A., and Beer, C.: Effects of bryophyte and lichen cover on permafrost
1290 soil temperature at large scale, *The Cryosphere*, 10(5), 2291–2315,
1291 <https://doi.org/10.5194/tc-10-2291-2016>, 2016.

Deleted: Peichl, M., Öquist, M., Löfvenius, M. O., Ilstedt, U., Sagerfors, J., Grelle, A., Lindroth, A., and Nilsson, M. B.: A 12-year record reveals pre-growing season temperature and water table level threshold effects on the net carbon dioxide exchange in a boreal fen, *Environ. Res. Lett.*, 9, 055006, <https://doi.org/10.1088/1748-9326/9/5/055006>, 2014. ¶

- 1299 Raczka, B., Duarte, H. F., Koven, C. D., Ricciuto, D.M., Thornton, P. E., Lin, J. C. and
 1300 Bowling, D. R.: An observational constraint on stomatal function in forests: evaluating
 1301 coupled carbon and water vapor exchange with carbon isotopes in the Community
 1302 Land Model (CLM4.5), *Biogeosciences*, 13(18), 5183-5204, DOI: 10.5194/bg-13-
 1303 5183-2016, 2016.
- 1304 Raghoebarsing, A. A., Smolders, A.J.P., Schmid, M.C., Rijpstra, W.I.C., Wolters-Arts,
 1305 M., Derksen, J., Jetten, M.S.M., Schouten, S., Sinninghe Damsté, J.S., Lamers,
 1306 L.P.M., Roelofs, J.G.M., Op den Camp, H.J.M., and Strous, M.: Methanotrophic
 1307 symbionts provide carbon for photosynthesis in peat bogs. *Nature*, 436, 1153-1156,
 1308 doi:10.1038/nature03802, 2005.
- 1309
 1310 Ricciuto, D. M., Sargsyan, K., and Thornton, P.E.: The Impact of Parametric
 1311 Uncertainties on Biogeochemistry in the E3SM Land Model, *J Adv Model Earth Sy*,
 1312 10(2), 297-319, doi: 10.1002/2017ms000962, 2018.
- 1313 Ricciuto, D.M., Xu, X., Shi, X., Wang, Y., Song, X., Schadt, C.W., Griffiths, N. A., Mao,
 1314 J., Warre, J.,M., Thornton, P.E., Chanton, J., Keller, J., Bridgman, S., Gutknecht, J.,
 1315 Sebestyen, S. D., Finzi, A., Kolka, R., and Hanson P.J.: An Integrative Model for Soil
 1316 Biogeochemistry and Methane Processes: I. Model Structure and Sensitivity Analysis,
 1317 *J. Geophys. Res.-Biogeo*, In review, 2019.
- 1318 Riutta, T., Laine, J., and Tuittila, E.-S.: Sensitivity of CO₂ exchange of fen ecosystem
 1319 components to water level variation, *Ecosystem*, 10(5), 718-733, 2007.
- 1320 Robroek, B.J.M., Limpens, J., Breeuwer, A., and Schouten, M.G.C.: Effects of water
 1321 level and temperature on performance of four Sphagnum mosses. *Plant*
 1322 *Ecology*, 190, 97-107, 2007.
- 1323 Robroek, B.J.M., Schouten, M.G.C., Limpens, J., Berendse F. and Poorter, H.: Interactive
 1324 effects of water table and precipitation on net CO₂ assimilation of three co-occurring
 1325 Sphagnum mosses differing in distribution above the water table, *Glob. Change Biol.*,
 1326 15, 680-691, 2009.
- 1327 Rosenzweig, C., Karoly, D., Vicarelli, M., Neofotis, P., Wu, Q., Casassa, G., Menzel, A.,
 1328 Root, T., Estrella, N., Seguin, B., Tryjanowski, P., Liu, C., Ravlins, S., and Imeson,
 1329 A.: Attributing physical and biological impacts to anthropogenic climate
 1330 change, *Nature*, 453, 353-357, doi:10.1038/nature06937, 2008.
- 1331 Rydin, H.: Effect of water level on desiccation of Sphagnum in relation to surrounding
 1332 Sphagna, *Oikos*, 45(3), 374-379, <https://doi:10.2307/3565573>, 1985.
- 1333 Rydin, H., and Clymo, R. S.: Transport of carbon and phosphorus-compounds about
 1334 Sphagnum. *Proceedings of the Royal Society Series B-Biological Sciences*,
 1335 237(1286), 63-84, <https://doi:10.1098/rspb.1989.0037>, 1989.
- 1336 Rousk, K., Rousk, J., Jones, D.L., Zackrisson, O., DeLuca, and T.H.: Feather moss
 1337 nitrogen acquisition across natural fertility gradients in boreal forests, *Soil Biol*
 1338 *Biochem*, 61, 86-95, 2013.

Formatted: Indent: Left: 0", Hanging: 0.19"

- 1339 Rousk, K., and Michelsen, A.: The sensitivity of Moss-Associated Nitrogen Fixation
 1340 towards Repeated Nitrogen Input, *Plos One*, 11(1), e0146655,
 1341 <https://doi.org/10.1371/journal.pone.0146655>, 2016.
- 1342 Rydsaa, J. H., Stordal, F., Bryn, A., and Tallaksen, L. M.: Effects of shrub and tree cover
 1343 increase on the near-surface atmosphere in northern Fennoscandia, *Biogeosciences*,
 1344 14, 4209-4227, <https://doi.org/10.5194/bg-14-4209-2017>, 2017.
- 1345 Saarnio, S., Jarvio, S., Saarinen, T., Vasander, H., Silvola, J.: Minor changes in
 1346 vegetation and carbon gas balance in a boreal mire under a raised CO₂ or NH₄NO₃
 1347 supply, *Ecosystems* 6:46-60, <https://doi.org/10.1007/s10021-002-0208-3>, 2003.
- 1348 Sargsyan, K., Safta, C., Najm, H. N., Debusschere, B. J., Ricciuto, D.M., and Thornton,
 1349 P.E.: Dimensionality Reduction for Complex Models Via Bayesian Compressive
 1350 Sensing, *International Journal for Uncertainty Quantification*, 4(1), 63-93, doi:
 1351 10.1615/Int.J.UncertaintyQuantification.2013006821, 2014.
- 1352 Sebestyén, S. D., Dorrance, C., Olson, D. M., Verry, E. S., Kolka, R. K., Elling, A. E.,
 1353 and Kyllander, R.: Long-term monitoring sites and trends at the Marcell Experimental
 1354 Forest, in: *Peatland biogeochemistry and watershed hydrology at the Marcell*
 1355 *Experimental Forest*, edited by: Kolka, R. K. Sebestyén, S. D., Verry, E. S., and
 1356 Brooks, CRC Press, New York, 15-71, 2011.
- 1357 Shi, X., Thornton, P. E., Ricciuto, D. M., Hanson, P. J., Mao, J., Sebestyén, S. D.,
 1358 Griffiths, N. A., and Bisht, G.: Representing northern peatland microtopography and
 1359 hydrology within the Community Land Model, *Biogeosciences*, 12(21), 6463-6477,
 1360 <https://doi.org/10.5194/bg-12-6463-2015>, 2015.
- 1361 Silva, L. C. R., Anand, M., and Leithead, M. D.: Recent widespread tree growth decline
 1362 despite increasing atmospheric CO₂, *PLoS ONE*, 5(7), e11543, doi:
 1363 10.1371/journal.pone.0011543, 2010.
- 1364
- 1365 Sonntag, O., Van Der Kamp, G., Barr, A.G., and Chen, J.: on the relationship between
 1366 water table depth and water vapor and carbon dioxide fluxes in a minerotrophic fen,
 1367 *Glob. Change Biol.*, 16(6), 1761-1776, [https://doi.org/10.1111/j.1365-](https://doi.org/10.1111/j.1365-2486.2009.02032.x)
 1368 2486.2009.02032.x, 2010.
- 1369 St-Hilaire, F., Wu, J., Roulet, N. T., Frolking, S., Lafleur, P. M., Humphreys, E. R., and
 1370 Arora, V.: McGill wetland model: evaluation of a peatland carbon simulator
 1371 developed for global assessments, *Biogeosciences*, 7, 3517-3530, 2010.
- 1372 Tarnocai, C.: The effect of climate change on carbon in Canadian peatlands, *Glob Planet*
 1373 *Change*, 53, 4, 222-232, 2006.
- 1374 Tenhunen, J.D., Weber, J.A., Yocum, C.S. and Gates, D.M.: Development of a
 1375 photosynthesis model with an emphasis on ecological applications, *Oecologia*, 26, 101-
 1376 119, 1976.
- 1377
- 1378 Tian, H., Lu, C., Yang, J., Banger, K., Huntzinger, D. N., Schwalm, C. R., Michalak, A.
 1379 M., Cook, R., Ciais, P., Hayes, D., Huang, M., Ito, A., Jacobson, A., Jain, A., Lei, H.,
 1380 Mao, J., Pan, S., Post, W.M., Peng, S., Poulter, B., Ren, W., Ricciuto, D.M., Schaefer, K.,
 1381 Shi, X., Tao, B., Wang, W., Wei, Y., Yang, Q., Zhang, B., and Zeng, N.: Global patterns

Formatted: Indent: Left: 0", Hanging: 0.19"

Deleted: Sulman, B. N., Desai, A. R., Saliendra, N. Z., Lafleur, P. M., Flanagan, L. B., Sonntag, O., Mackay, D. S., Barr, A. G., and Kamp, G. V. D.: CO₂ fluxes at northern fens and bogs have opposite responses to inter-annual fluctuations in water table, *Geophys. Res. Lett.*, 37, L19702, doi:10.1029/2010GL044018, 2010.

1388 of soil carbon stocks and fluxes as simulated by multiple terrestrial biosphere models:
1389 sources and magnitude uncertainty, *Global Biogeochem Cycles*, 29, 775-792,
1390 doi:10.1002/2014GB005021, 2015.

1391 Titus, J. E., Wagner, D.J., and Stephens, M.D.: Contrasting Water Relations of
1392 Photosynthesis for 2 Sphagnum Mosses, *Ecology*, 64, 1109-1115, 1983.

1393 Todd-Brown, K. E. O., Randerson, J. T., Post, W. M., Hoffman, F. M., Tarnocai, C.,
1394 Schuur, E. A. G., and Allison, S. D.: Causes of variation in soil carbon simulations
1395 from CMIP5 Earth system models and comparison with observations, *Biogeosciences*,
1396 10, 1717–1736, doi:10.5194/bg-10-1717-2013, 2013.

1397 Toet, S., Cornelissen, J.H., Aerts, R., van Logtestijn, R.S., de Beus, M., Stoevelaar, R.:
1398 Moss responses to elevated CO₂ and variation in hydrology in a temperate lowland
1399 peatland. *Plants and climate change*. Springer, Netherlands, pp 27-42, 2006.

1400 Turetsky, M. R., Wieder, R. K., and Vitt, D. H.: Boreal peatland C fluxes under varying
1401 permafrost regimes, *Soil Biol. Biochem.*,34,907-912, 2002.

1402 Turetsky, M. R., and Wieder, R. K.: Boreal bog Sphagnum refixes soil-produced and
1403 respired 14CO₂, *Ecoscience*, 6(4), 587-591.
1404 <https://doi:10.1080/11956860.1999.11682559>, 1999.

1405 Turetsky, M.R., Mack, M.C., Hollingsworth, T.N., and Harden, J.W.: The role of mosses
1406 in ecosystem succession and function in Alaska's boreal forest, *Canadian Journal of*
1407 *Forest Research* 4, 1237-1264, 2010.

1408 Turetsky, M. R., Bond-Lamberty, B., Euskirchen, E., Talbot, J., Frohling, S., McGuire,
1409 A. D., and Tuittila, E.-S.: The resilience and functional role of moss in boreal and arc-
1410 tic ecosystems, *New Phytol.*, 196, 49-67, doi:10.1111/j.1469- 8137.2012.04254.x,
1411 2012.

1412

1413 Van, B. N.: How Sphagnum bogs down other plants, *Trends Ecol. Evol*, 10, 270-275,
1414 1995.

1415 Van Der Heijden, E., Verbeek, S.K., Kuiper, P.J.C.: Elevated atmospheric CO₂ and
1416 increased nitrogen deposition: effects on C and N metabolism and growth of the peat
1417 moss *Sphagnum recurvum* P. Beauv. var. *mucronatum* (Russ.), *Warnst. Glob Change*
1418 *Biol* 6, 201 – 212, <https://doi.org/10.1046/j.1365-2486.2000.00303.x>, 2000.

1419 van der Schaaf, S.: Bog hydrology, in: *Conservation and Restoration of Raised Bogs:*
1420 *Geological, Hydrological and Ecological Studies*, edited by: Schouten, M.G.C., The
1421 Government Stationery Office, Dublin, 54-109, 2002.

1422 van der Wal, R., Pearce, I.S.K and Brooker, R.W.: Mosses and the struggle for light in a
1423 nitrogen-polluted world, *Oecologia*, 142,159-68, 2005.

1424 Van Gaalen, K. E., Flanagan, L. B., and Peddle, D. R.: Photosynthesis, chlorophyll
1425 fluorescence and spectral reflectance in Sphagnum moss at varying water contents,
1426 *Oecologia*, 153(1), 19-28, doi:10.1007/s00442-007-0718-y, 2007.

Formatted: Indent: Left: 0", Hanging: 0.19"

Formatted: Indent: Left: 0", Hanging: 0.19"

Formatted: Indent: Left: 0", Hanging: 0.19"

Formatted: Indent: Left: 0", Hanging: 0.19", Line spacing: single

- 1427 Verry, E. S., and Janssens, J.: Geology, vegetation, and hydrology of the S2 bog at the
1428 MEF: 12,000 years in northern Minnesota, in *Peatland biogeochemistry and watershed*
1429 *hydrology at the Marcell Experimental Forest*, edited by R. K. Kolka S. D.
1430 Sebestyen, E. S. Verry, K.N. Brooks, CRC Press, New York, 93-134, 2011.
- 1431 Vile, M. A., Kelman Wieder, R., Živković, T., Scott, K. D., Vitt, D. H., Hartsock, J. A.,
1432 Iosue, C. L., Quinn, J.C., Petix, M., Fillingim, H.M., Popma, J.M.A., Dynarski, K.A.,
1433 Jackman, T. R., Albright, C.M., and Wykoff, D. D. : N₂-fixation by methanotrophs
1434 sustains carbon and nitrogen accumulation in pristine peatlands, *Biogeochemistry*,
1435 121, 317-328, <https://doi.org/10.1007/s10533-014-0019-6>, 2014.
- 1436 Vitt, D. H.: A key and review of bryophytes common in North American peatlands,
1437 *Evansia*, 31, 121-158, 2014.
- 1438 Wania, R., Ross, I., Prentice, I.C.: Integrating peatlands and permafrost into a dynamic
1439 global vegetation model: 1. Evaluation and sensitivity of physical land surface
1440 processes, *Global Biogeochem. Cycles* 23, GB3014, doi:10.1029/2008GB003412,
1441 2009.
- 1442 Wania, R., Melton, J. R., Hodson, E. L., Poulter, B., Ringeval, B., Spahni, R., Bohn, T.,
1443 Avis, C. A., Chen, G., Eliseev, A. V., Hopcroft, P. O., Riley, W. J., Subin, Z. M., Tian,
1444 H., van Bodegom, P.M., Kleinen, T., Yu, Z., Singarayer, J. S., Zurcher, S.,
1445 Lettenmaier, D. P., Beerling, D. J., Denisov, S. N., Prigent, C., Papa, F., and Kaplan, J.
1446 O.: Present state of global wetland extent and wetland methane modelling:
1447 methodology of a model inter-comparison project (WETCHIMP), *Geosci. Model*
1448 *Dev.*, 6, 617-641, 2013.
- 1449 Walker, M.D., Wahren, C.H., Hollister, R.D., Henry, G.H.R., Ahlquist, L.E., Alatalo,
1450 J.M., Bret-Harte, M.S., Calef, M.P., Callaghan, T.V., Carroll, A.B., Epstein, H.E.,
1451 Jonsdottir, I.S., Klein, J.A., Magnusson, B., Molau, U., Oberbauer, S.F., Rewa, S.P.,
1452 Robinson, C.H., Shaver, G.R., Suding, K.N., Thompson, C.C., Tolvanen, A., Totland,
1453 O., Turner, P.L., Tweedie, C.E., Webber, and P.J., Wookey, P.A.: Plant community
1454 responses to experimental warming across the tundra biome, *Proc Natl Acad Sci USA*,
1455 10,31342-6, 2006.
- 1456 Walker, T. N., Ward, S. E., Ostle, N. J., and Bardgett, R. D.: Contrasting growth
1457 responses of dominant peatland plants to warming and vegetation composition,
1458 *Oecologia*, 178, 141-151, <https://doi.org/10.1007/s00442-015-3254-1>, 2015.
- 1459 Walker, A. P., Carter, K. R., Gu, L., Hanson, P. J., Malhotra, A., Norby, R.J., Sebestyen,
1460 S. D., Wullschleger, S. D., Weston, D. J.: 2017. Biophysical drivers of seasonal
1461 variability in Sphagnum gross primary production in a northern temperate bog, *J.*
1462 *Geophys. Res.-Biogeo*, 122, 1078-1097, <https://doi.org/10.1002/2016JG003711>, 2017.
- 1463 Wang, H., Richardson, C. J., and Ho, M.: Dual controls on carbon loss during drought in
1464 peatlands, *Nature Climate Change*, 5, 58- 587, 2015.

- 1465 Ward, S. E., Ostle, N. J., Oakley, S., Quirk, H., Henrys, P. A., and Bardgett, R. D.:
1466 Warming effects on greenhouse gas fluxes in peatlands are modulated by vegetation
1467 composition, *Ecol. Lett.*, 16, 1285-1293, 2013.
- 1468 Weltzin, J. F., Harth, C., Bridgman, S. D., Pastor, J., and Vonderharr, M.: Production and
1469 microtopography of bog bryophytes: response to warming and water-table
1470 manipulations, *Oecologia*, 128(4), 557-565, [https://doi:10.1007/s004420100691](https://doi.org/10.1007/s004420100691), 2001.
1471 Weston, D.J., Timm, C.M., Walker, A.P., Gu, L., Muchero, W., Schmuta, J., Shaw, A. J.,
1472 Tuskan, G. A., Warren, J.M., and Willschleger, S.D.: Sphagnum physiology in the
1473 context of changing climate: Emergent influences of genomics, modeling and host-
1474 microbiome interactions on understanding ecosystem function, *Plant, Cell and*
1475 *Environment*, 38, 1737-1751, doi: 10.1111/pce.12458, 2015.
- 1476 White, M. A., Thornton, P. E., Running, S. W., and Nemani, R. R.: Parameterization and
1477 sensitivity analysis of the BIOME-BGC terrestrial ecosystem model: Net primary
1478 production controls, *Earth Interactions*, 4(3), 1-85, 2000.
- 1479 Wieder R. K.: Primary production in boreal peatlands. In: *Boreal peatland ecosystems*,
1480 edited by: Wieder, R. K., and Vitt, D. H., Springer-Verlag, Berlin Heidelberg,
1481 Germany, 145-163, 2006.
- 1482 Wiley, E., Rogers, B. J., Griesbauer, H. P., and Landhausser, S. M.: Spruce shows greater
1483 sensitivity to recent warming than Douglas-fir in central British Columbia, *Ecosphere*
1484 9(5), e02221, 10.1002/ecs2.2221, 2018
1485 Williams T.G. and Flanagan, L.B.: Measuring
1486 and modelling environmental influences on photosynthetic gas exchange in Sphagnum
and Pleurozium, *Plant Cell and Environment*, 21, 555-564, 1998.
- 1487 Williams T.G. & Flanagan L.B.: Measuring and modelling environmental influences on
1488 photosynthetic gas exchange in *Sphagnum* and Pleurozium, *Plant Cell and*
1489 *Environment*, 21, 555-564, 1998.
- 1490 Wilmking, M., Juday, G. P., Barber, V. A., and Zald, H. S. J.: Recent climate warming
1491 forces contrasting growth responses of white spruce at treeline in Alaska through
1492 temperature thresholds, *Glob. Change Biol.* 10, 1724-1736, 2004.
- 1493 Wolf, A., Callaghan, T. V., and Larson, K.: Future changes in vegetation and ecosystem
1494 function of the Barents Region, *Climatic Change*, 87, 51-73,
1495 <https://doi.org/10.1007/s10584-007-9342-4>, 2008.
- 1496 Wolken, J. M., Mann, D. H., Grant, T. A., Lloyd, A. H., Rupp, T.S., and Hollingsworth,
1497 T. N.: 2016. Climate-growth relationships along a black spruce topose-quence in
1498 interior Alaska, *Arctic, Antarctic, and Alpine Research*, 48, 637-652, 2016.
1499
- 1500 Wu, J., Roulet, N. T., Sagerfors, J., Nilsson, M. B.: Simulation of six years of carbon
1501 fluxes for a sedge-dominated oligotrophic minerogenic peatland in Northern Sweden
1502 using the McGill Wetland Model (MWM), *J. Geophys. Res. -Biogeosciences*,
1503 doi:10.1002/jgrg.20045, 2013.

Formatted: Indent: Left: -0.06", Line spacing: single

1504 Wu, Y. and Blodau, C.: PEATBOG: a biogeochemical model for analyzing coupled
1505 carbon and nitrogen dynamics in northern peatlands, *Geosci. Model Dev.*, 6, 1173-
1506 1207, doi:10.5194/gmd-6-1173-2013, 2013.

1507 Wu, J. and Roulet, N. T.: Climate change reduces the capacity of northern peatlands to
1508 absorb the atmospheric carbon dioxide: The different responses of bogs and fens,
1509 *Global Biogeochem. Cycles*, doi.org/10.1002/2014GB004845, 2014.

1510 Wu, Y., Verseghy, D. L., and Melton, J. R.: Integrating peatlands into the coupled
1511 Canadian Land Surface Scheme (CLASS) v3.6 and the Canadian Terrestrial
1512 Ecosystem Model (CTEM) v2.0, *Geosci. Model Dev.*, 9, 2639-2663,
1513 doi:10.5194/gmd-9-2639-2016, 2016.

1514 Yang, X., Ricciuto, D. M., Thornton, P. E., Shi, X., Xu, M., Hoffman, F., Norby R. J.:
1515 The effects of phosphorus cycle dynamics on carbon sources and sinks in the Amazon
1516 region: a modeling study using ELM v1, *J. Geophys. Res.-Biogeo*, 124,
1517 <https://doi.org/10.1029/2019JG005082>, 2019.

1518 Yu, Z., Loisel, J., Brosseau, D. P., Beilman, D. W., and Hunt, S.J.: Global peatland
1519 dynamics since the Last Glacial Maximum, *Geophys. Res. Lett.*, 37, L13402,
1520 doi:10.1029/2010GL043584, 2010.

1521 Yurova, A., Wolf, A., Sagerfors, J., and Nilsson, M.: Variations in net ecosystem
1522 exchange of carbon dioxide in a boreal mire: Modeling mechanisms linked to water
1523 table position, *J. Geophys. Res.-Biogeo.*, 112, G02025, doi:10.1029/2006JG000342,
1524 2007

1525 Zhang, W. X., Miller, P. A., Smith, B., Wania, R., Koenigk, T., and Doscher, R.: Tundra
1526 shrubification and tree-line advance amplify arctic climate warming: results from an
1527 individual- based dynamic vegetation model, *Environ. Res. Lett.*, 8, 034023,
1528 <https://doi.org/10.1088/1748-9326/8/3/034023>, 2013.

1529 Zhuang, Q., Melillo, J.M., Sarofim, M.C., Kicklighter, D.W., McGuire, A.D., Felzer,
1530 B.S., Sokolov, A., Prinn, R.G., Steudler, P.A., and Hu, S.: CO₂ and CH₄ exchanges
1531 between land ecosystems and the atmosphere in northern high latitudes over the 21st
1532 century, *Geophys. Res. Lett.*, 33, L17403, doi:10.1029/2006GL026972, 2006.
1533
1534